RESEARCH ARTICLE

Cerebellar Output Controls Generalized Spike-and-Wave Discharge Occurrence

Lieke Kros, PhD,[1] Oscar H. J. Eelkman Rooda, MD, MSc,[1] Jochen K. Spanke, MSc,[1] Parimala Alva, MSc,[2] Marijn N. van Dongen, PhD,[3] Athanasios Karapatis, BEng,[3] Else A. Tolner, PhD,[4] Christos Strydis, PhD,[1] Neil Davey, PhD,[2] Beerend H. J. Winkelman, PhD,[5] Mario Negrello, PhD,[1] Wouter A. Serdijn, PhD,[3] Volker Steuber, PhD,[2] Arn M. J. M. van den Maagdenberg, PhD,[4,6] Chris I. De Zeeuw, MD, PhD,[1,5] and Freek E. Hoebeek, PhD[1]

Objective: Disrupting thalamocortical activity patterns has proven to be a promising approach to stop generalized spike-and-wave discharges (GSWDs) characteristic of absence seizures. Here, we investigated to what extent modulation of neuronal firing in cerebellar nuclei (CN), which are anatomically in an advantageous position to disrupt cortical oscillations through their innervation of a wide variety of thalamic nuclei, is effective in controlling absence seizures.
Methods: Two unrelated mouse models of generalized absence seizures were used: the natural mutant *tottering*, which is characterized by a missense mutation in *Cacna1a*, and inbred *C3H/HeOuJ*. While simultaneously recording single CN neuron activity and electrocorticogram in awake animals, we investigated to what extent pharmacologically increased or decreased CN neuron activity could modulate GSWD occurrence as well as short-lasting, on-demand CN stimulation could disrupt epileptic seizures.
Results: We found that a subset of CN neurons show phase-locked oscillatory firing during GSWDs and that manipulating this activity modulates GSWD occurrence. Inhibiting CN neuron action potential firing by local application of the γ-aminobutyric acid type A (GABA-A) agonist muscimol increased GSWD occurrence up to 37-fold, whereas increasing the frequency and regularity of CN neuron firing with the use of GABA-A antagonist gabazine decimated its occurrence. A single short-lasting (30–300 milliseconds) optogenetic stimulation of CN neuron activity abruptly stopped GSWDs, even when applied unilaterally. Using a closed-loop system, GSWDs were detected and stopped within 500 milliseconds.
Interpretation: CN neurons are potent modulators of pathological oscillations in thalamocortical network activity during absence seizures, and their potential therapeutic benefit for controlling other types of generalized epilepsies should be evaluated.

ANN NEUROL 2015;77:1027–1049

Absence epilepsy is among the most prevalent forms of generalized epilepsy among children and is characterized by sudden periods of impaired consciousness and behavioral arrest.[1,2] Like other types of generalized epilepsies, absence seizures are electrophysiologically defined by oscillatory activity in cerebral cortex and the thalamic complex.[3] Thalamocortical oscillations are primarily caused by excessive cortical activity and can be identified in the electrocorticogram (ECoG) as generalized spike-and-wave discharges (GSWDs).[3,4] The underlying excessive cortical activity not only excites thalamic neurons, but also provides potent bisynaptic inhibition

View this article online at wileyonlinelibrary.com. DOI: 10.1002/ana.24399

Received Nov 7, 2014, and in revised form Mar 2, 2015. Accepted for publication Mar 3, 2015.

Address correspondence to Dr Hoebeek, Department of Neuroscience, Erasmus MC, Wytemaweg 80, 3015 CN, Rotterdam, the Netherlands. E-mail: f.hoebeek@erasmusmc.nl

From the [1]Department of Neuroscience, Erasmus Medical Center, Rotterdam, the Netherlands; [2]Science and Technology Research Institute, University of Hertfordshire, Hatfield, United Kingdom; [3]Bioelectronics Section, Faculty of Electrical Engineering, Mathematics, and Computer Science, Delft University of Technology, Delft, the Netherlands; [4]Department of Neurology, Leiden University Medical Center, Leiden, the Netherlands; [5]Netherlands Institute for Neuroscience, Royal Dutch Academy for Arts and Sciences, Amsterdam, the Netherlands; and [6]Department of Human Genetics, Leiden University Medical Center, Leiden, the Netherlands

Additional Supporting Information may be found in the online version of this article.

by means of cortical axonal collaterals to the inhibitory reticular thalamic nucleus.[3,5–7] Excess tonic γ-aminobutyric acid (GABA)-mediated inhibition in thalamus may also contribute to absence seizures.[3,7,8] Oscillatory cortical activity thereby poses a dual excitation–inhibition effect on thalamic neurons, which drives thalamocortical network oscillations.[5,7–9]

Recent studies in several rodent models indicate that direct stimulation of thalamic nuclei[10] or cerebral cortex[11] can be effective in disrupting thalamocortical oscillations and thereby stopping generalized oscillations in thalamocortical networks, such as GSWDs. Apart from direct interventions in thalamus and cortex, thalamic afferents can affect the balance in excitation and inhibition and thereby potentially mediate thalamocortical oscillations. One of the initial stimulation sites to prevent seizures in epileptic patients was the cerebellar cortex.[12–18] Yet, as shown in 3 controlled, blind studies,[19–21] the impact of these cerebellar surface stimulations was highly variable and probably reflects irregularities in the converging inputs from superficial and deeper parts of the cerebellar cortex neurons to the cerebellar nuclei (CN).[22]

Given the considerable divergence of excitatory axonal projections from the CN to a wide range of motor, associative, and intralaminar thalamic nuclei,[4,6,23–29] we considered this region an ideal candidate to effectively modulate thalamocortical oscillations. We hypothesized that altering the firing patterns of CN neurons should affect GSWD occurrence. To test this hypothesis, we utilized homozygous *tottering* (*tg*) mice that frequently show absence seizures and harbor a P601L missense mutation in the *Cacna1a* gene that encodes the pore-forming α_{1A}-subunit of voltage-gated $Ca_V2.1$ Ca^{2+} channels.[30,31] Once we established that *tg* CN neurons showed oscillatory action potential firing patterns comparable to that found in rat models for absence epilepsy,[32] we assessed the effect of increasing or decreasing CN neuronal firing on GSWD occurrence by local pharmacological interventions using modulators of $GABA_A$-mediated neurotransmission. In addition, we generated a closed-loop detection system for on-demand optogenetic stimulation to stimulate CN neurons with millisecond precision. Finally, to exclude the possibility that our design of intervention is tailored to the specific pathophysiology of *tg* mice, we extended our key experiments to an unrelated mouse model for absence epilepsy: the *C3H/HeOuJ* inbred mouse line.[33]

Materials and Methods

All experiments were performed in accordance with the European Communities Council Directive. Protocols were reviewed and approved by local Dutch experimental animal committees.

Animals

Data were collected from 4- to 30-week-old homozygous and wild-type littermates of natural mutant *tg* mice and 8- to 10-week-old inbred *C3H/HeOuJ* mice. Male and female *tg* and wild-type littermates were bred using heterozygous parents. The colony, which was originally obtained from Jackson Laboratory (Bar Harbor, ME), was maintained in *C57BL/6NHsd* purchased from Harlan Laboratories (Horst, the Netherlands). Conformation of the presence of the *tg* mutation in the *Cacna1a* gene was obtained by polymerase chain reaction using 5′-TTCTGGGTACCAGATACAGG-3′ (forward) and 5′-AAGTGTCGAAGTTGGTGCGC-3′ (reverse) primers (Eurogentech, Seraing, Belgium) and subsequent digestion using restriction enzyme *NsbI* at the age of postnatal day (P) 9 to P12. Male inbred *C3H/HeOuJ* mice were purchased from Charles River Laboratories (Wilmington, MA).

Experimental Procedures

SURGERY. Mice were anesthetized with isoflurane (4% in 0.5l/min O_2 for induction and 1.5% in 0.5l/min O_2 for maintenance). The skull was exposed, cleaned, and treated with OptiBond All-In-One (Kerr Corporation, Orange, CA) to ensure adhesion of a light-curing hybrid composite (Charisma; Heraeus Kulzer, Hanau, Germany) to the skull to form a pedestal. Subsequently, five 200μm Teflon-coated silver ball tip electrodes (Advent Research Materials, Eynsham, UK) or five 1mm stainless steel screws were subdurally implanted for cortical recordings by ECoG. Four of the electrodes were bilaterally positioned above the primary motor cortex (+1mm anterior-posterior [AP]; ±1mm medial - lateral [ML] relative to bregma) and primary sensory cortex (−1mm AP; ± 3.5mm ML). A fifth electrode was placed in the rostral portion of the interparietal bone to serve as reference (−1mm AP relative to lambda). The electrodes and their connectors were fixed to the skull and embedded in a pedestal composed of the hybrid composite or dental acrylic (Simplex Rapid; Associated Dental Products, Kemdent Works, Purton, UK). To enable optogenetic control of neuronal activity in CN, a subset of *tg* and *C3H/HeOuJ* mice received 2 small (∼0.5mm in diameter) craniotomies in the interparietal bone (−2mm AP relative to lambda; ±1.5–2mm ML) to initially accommodate the injection pipette and later the optical fibers. CN were stereotactically injected bilaterally with 100 to 120nl of the AAV2-hSyn-ChR2(H134R)-EYFP vector (kindly provided by Dr K. Deisseroth [Stanford University] through the Vector Core at the University of North Carolina) at a rate of ∼20nl/min 3 to 6 weeks prior to recordings. To allow electrophysiological recordings from CN neurons, all mice received bilateral craniotomies (∼2mm diameter) in the occipital bone without disrupting the dura mater. Finally, a dental acrylic recording chamber (Simplex rapid) was constructed. The exposed tissue was covered with tetracycline-containing ointment (Terra-cortril; Pfizer, New York, NY) and the recording chamber was sealed with bone wax (Ethicon, Somerville, NJ). After surgery, the mice recovered for at least 5 days (or 3 weeks in the case of virally injected

mice) in their home cage and were allowed two ~3-hour sessions on consecutive days during which the mice were left undisturbed to accommodate to the setup.

ELECTROPHYSIOLOGICAL RECORDINGS. During the accommodation session, the animals' motor behavior was visually inspected for behavioral correlates of the oscillatory cortical activity during episodes of GSWDs. No consistent patterns of movement were identified during such epileptic activity, as described before in *tg* and other rodent models of absence epilepsy.[30,32,34] Recordings were performed in awake, head-fixed animals, lasted no longer than 4 consecutive hours, and were performed during various times of day. No consistent pattern was identified in ECoG frequency spectra with respect to the day–night cycle.[35] While being head-restrained, mice were able to move all limbs freely. Body temperature was supported using a homeothermic pad (FHC, Bowdoin, ME). For extracellular single unit recordings, custom-made, borosilicate glass capillaries (outer diameter = 1.5mm, inner diameter = 0.86mm, resistance = 8–12MΩ, taper length = ~8mm, tip diameter = ~1μm; Harvard Apparatus, Holliston, MA) filled with 2M NaCl were positioned stereotactically using an electronic pipette holder (SM7; Luigs & Neumann, Ratingen, Germany). CN were localized by stereotactic location as well as the characteristic sound and density of neuronal activity.[36] To record from medial CN (MCN), electrodes were advanced through vermal lobules 6 to 7 with 0° jaw angle relative to the interaural axis to a depth of 1.6 to 2.4mm. To record from interposed nuclei (IN), electrodes were advanced through the paravermal or hemispheric part of lobules 6 to 7 using a yaw angle of ~10° relative to the interaural axis to a depth of 1.8 to 2.7mm. To record from lateral CN (LCN), electrodes were advanced through the paravermal or hemispheric part of lobules 6 to 7 using a yaw angle of ~25° relative to the interaural axis to a depth of 2.7 to 4mm. A subset of electrophysiological recording sites was identifiable following Evans blue injections (see below) and confirmed the accuracy of our localization technique. ECoGs were filtered online using a 1 to 100Hz band pass filter and a 50Hz notch filter. Single unit extracellular recordings and ECoGs were simultaneously sampled at 20kHz (Digidata 1322A; Molecular Devices, Axon Instruments, Sunnyvale, CA), amplified, and stored for offline analysis (CyberAmp & Multiclamp 700A, Molecular Devices).

PHARMACOLOGICAL MODULATION OF CN NEURONAL ACTION POTENTIAL FIRING. To bilaterally target the CN for pharmacological intervention, their location was first determined as described above, after which we recorded 1 hour of "baseline" ECoG. Next, a borosilicate glass capillary (Harvard Apparatus; tip diameter = ~5μm) filled with 1 of the following mixtures replaced the recording pipette to allow high spatial accuracy of the injection: to decrease CN neuronal action potential firing, we applied 0.5% muscimol ($GABA_A$-agonist; Tocris Bioscience, Bristol, UK) dissolved in 1M NaCl (Sigma-Aldrich, St Louis, MO); to increase CN neuronal action potential firing, we applied 100μM gabazine ($GABA_A$- antagonist; Tocris) dissolved in 1M NaCl; or 1M NaCl for sham injections. The experimenter was blinded for the solutions injected. The solution was bilaterally administered to CN by pressure injections of ~150nl at a rate of ~50nl/min, following which 1 hour of postinjection ECoG was recorded. As an additional control, similarly sized injections of saline with either gabazine or muscimol were administered to lobules 6 and 7 and Crus I and Crus II of the cerebellar cortex. The drugs were injected superficially (0.7–1mm from the surface) to avoid spread to the CN. The locations of the injections were identified with the use of electrophysiological recordings and stereotactic coordinates, and most (19 of 26) CN injections were histologically confirmed using the fluorescence of Evans blue (1% in 1M saline supplied to the injected solution; Supplementary Fig).[37] To verify the effects of muscimol, gabazine, and vehicle, we recorded extracellular activity in the injected area during 20 to 50 minutes after the injections. Immediately after acquiring the postinjection ECoG, an overdose of sodiumpentobarbital (0.15ml intraperitoneally) was administered allowing transcardial perfusion (0.9% NaCl followed by 4% paraformaldehyde in 0.1M phosphate buffer [PB]; pH = 7.4) to preserve the tissue for histological verification of the injections.

OPTOGENETIC STIMULATION OF CN NEURONS. Optic fibers (inner diameter = 200μm, numerical aperture = 0.39; Thor labs, Newton, NJ, USA) were placed ~200μm from the injection site and connected to 470nm or 590nm light-emitting diodes (LEDs; Thor labs), or ~200μm above the brain, that is, in the "wrong location." Light intensity at the tip of the implantable fiber was $550 \pm 50\mu W/mm^2$ (measured after each experiment). Activation of LEDs by a single 30- to 300-millisecond pulse was triggered manually (open-loop) or by a closed-loop detection system (as described below). In each mouse, 4 stimulation protocols were used: (1) bilateral stimulation (470nm), (2) unilateral stimulation (470nm), (3) bilateral stimulation (590nm), and (4) bilateral stimulation (470nm) with optical fibers outside of the CN (to exclude potential effects of visual input on the GSWD occurrence.[30,32] After the last experimental session, animals were sedated and perfused (as described above) to preserve tissue for histological verification of channelrhodopsin-2 (ChR2) expression.

IMMUNOFLUORESCENCE. After perfusion, the cerebellum was removed and postfixed in 4% paraformaldehyde in 0.1M PB for 1.5 hour, placed in 10% sucrose in 0.1M PB at 4°C overnight, and subsequently embedded in gelatin in 30% sucrose (in 0.1M PB). Embedded brains were postfixed for 2.5 to 3 hours in 30% sucrose and 10% formaldehyde (in Milli-Q; Millipore, Billerica, MA) and placed overnight in 30% sucrose (in 0.1M PB) at 4°C. Forty-micrometer-thick transversal slices were serially collected for immunofluorescent 4′,6-diamidino-2-phenylindole (DAPI) staining. To confirm correct localization of the injections, fluorescence was assessed with images captured using a confocal laser scanning microscope (LSM 700; Zeiss, Lambrecht, Germany) at 555nm (Evans blue), 405nm (DAPI), and 488 to 527nm (green fluorescent protein/yellow fluorescent protein range) and optimized for contrast and brightness

manually (Zen 2009 software, Zeiss). The fluorescent images were captured using a tile-scan function of the Zen software with a ×10 objective and have been optimized for representation using Adobe Illustrator (Creative Suite 6; Adobe Systems, San Jose, CA).

Data Analyses

OFFLINE GSWD DETECTION. To accurately determine start and end of absence GSWDs and the locations of ECoG spikes (negative ECoG peaks during episodes of GSWDs), a custom-written GSWD detection algorithm (LabVIEW, National Instruments, Austin, TX) was used. In short, we detected those time points in the ECoG for which the first derivative of the filtered ECoG traces (3rd order Butterworth 1Hz high pass) changed polarity. The amplitude differences between each point and both its neighbors were summed to detect fast, continuous amplitude changes and potential GSWDs with a manually set amplitude threshold. Series of GSWDs were marked when: (1) 5 threshold-exceeding data points appeared within 1 second and (2) each of the intervals between the points was <300 milliseconds. Furthermore, we separated GSWDs by applying the following 4 rules: (1) a point is the first spike of a GSWD episode if there are no other spikes in the previous 300 milliseconds, (2) a point is the last spike of a GSWD episode if there are no other spikes in the next 350 milliseconds, (3) the inter-GSWD episode interval is ≥1 second, and (4) the minimal GSWD duration is 1 second.

GSWD DEFINITION. An ictal period is defined as starting at the first ECoG spike of a GSWD and ending at the last ECoG spike. Unless stated otherwise, spike-and-wave discharges that lasted >1 second and appeared in both M1 and S1 were considered GSWDs.

An interictal period is defined as the time in between GSWDs starting 2 seconds after 1 GSWD and ending 2 seconds before the next GSWD.

DETECTION OF ACTION POTENTIALS IN EXTRACELLULAR RECORDINGS. Extracellular recordings were included if activity was well isolated and held stable for >100 seconds. Action potential detection in extracellular traces was performed using threshold-based analyses with customized MATLAB (MathWorks, Natick, MA) routines incorporating principal component analysis of the spike waveform or with the MATLAB-based program SpikeTrain (Neurasmus, Erasmus MC Holding, Rotterdam, the Netherlands).

GSWD-RELATED FIRING PATTERN MODULATION. A custom-written algorithm in LabVIEW was used to assess whether CN neurons showed GSWD-modulated firing patterns during GSWDs in the ECoG of the contralateral primary sensory cortex (in the case of medial CN neurons) or primary motor cortex (in the case of interposed or lateral CN neurons). The minimum duration per episode was set at 2 seconds to construct GSWD-triggered raster plots and peri-GSWD time histograms (PSTHs) with a 5-millisecond bin width, which allowed us to determine: (1) modulation amplitude: the amplitude difference between the peak and trough near t = 0; (2) modulation frequency: frequency of the sine wave that fits the PSTH best; and (3) mean power at GSWD frequency: a fast Fourier transform (fft) between 6 and 9Hz (GSWD frequency range). Next, the interspike intervals (ISIs) used for this PSTH were randomly shuffled 500 times and converted into a new PSTH with 5-millisecond bin width to create normal distributions of modulation amplitude and mean power at GSWD frequency. Z scores were calculated for the real and shuffled data by applying: $Z = (X - \mu)/\sigma$, where X = the value based on the original PSTH, μ = the mean of the bootstrapped normal distribution, and σ = its standard deviation (SD). Cells were identified as GSWD modulated if: (1) the modulation amplitude was significantly higher than expected by chance ($Z \geq 1.96$, $p \leq 0.05$), (2) the cell modulated at GSWD frequency (6–9Hz), and (3) the mean power at GSWD frequency was significantly higher than expected by chance ($Z \geq 1.96$, $p \leq 0.05$). Because all CN neurons that showed significant Z scores of mean power at GSWD frequency also showed significantly higher modulation amplitudes, the former was used for further analyses. The term Z score refers to mean power at GSWD frequency unless stated otherwise.

COHERENCE. To determine the spectral coherence between the activity of a CN neuron and the ECoG signal during GSWDs, a custom-written MATLAB routine was used. The extracellular signal was time-binned at 1-millisecond precision, convolved with a sinc(x)-kernel (cutoff frequency = 50Hz) and downsampled to 290 Hz. The ECoG signal was directly downsampled to 290 Hz. The magnitude squared coherence was calculated per GSWD episode using Welch's averaged, modified periodogram method and is defined as: $C_{xy}(f) = |P_{xy}(f)|^2 / P_{xx}(f) * P_{yy}(f)$ with the following parameters: window = 290 (Hamming), noverlap = 75%, length of fft (nfft) = 290, sampling frequency = 290 (due to the window size, only GSWDs > 1.5 seconds were considered). The coherence value per GSWD was defined as the maximum coherence in the 6 to 9Hz frequency band; a weighted average per cell based on GSWD duration was used.

FIRING PATTERN PARAMETERS. Firing patterns parameters were assessed using custom-written LabVIEW-based programs calculating firing frequency, coefficient of variation (CV) of ISIs = σ_{ISI}/μ_{ISI}, $CV2 = 2|ISI_{n+1} - ISI_n|/(ISI_{n+1} + ISI_n)$, and burst index = number of action potentials within bursts/total number of action potentials in a recording, where a burst is defined as ≥3 consecutive action potentials with an ISI ≤ 10 milliseconds. CV reports regularity of firing throughout the whole recording and CV2 quantifies the regularity of firing on a spike-to-spike basis.[38] Firing pattern parameters were specifically calculated for ictal and interictal periods.

REGRESSION ANALYSES OF INTERICTAL CN ACTIVITY. To evaluate whether there is a type of CN neuron that is predisposed for ictal phase-locking during GSWDs, we analyzed the neurons' interictal activity using a custom-made MATLAB routine, aiming to probe the predictability of the ictal activity. We used Gaussian process regression,[39] which is

considered to be among the best nonlinear regression methods, to determine whether the GSWD modulation of the activity was predictable from the interictal activity of the neurons. The measures that enabled the prediction of the modulation amplitude most accurately were CV, log-interval entropy, firing frequency, and permutation entropy. The interictal parts of the extracellular recordings were divided into 1-second bins. To calculate the log-interval entropy, in which entropy measures the predictability of a system, first a natural logarithm of the intervals, in milliseconds, was taken to construct a histogram with a bin width of 0.02 log_e (time). Furthermore, a Gaussian convolution was performed using a kernel of one-sixth SD of the *log*(ISIs).

The entropy of the ISI histogram $p(I_i)$ was calculated by:

$$\mathrm{Ent(I)} = -\sum_{i=1}^{N} \mathrm{p(I_i)log_2p(I_i)} \qquad (1)$$

Furthermore, we analyzed the permutation entropy, which is calculated as the predictability of the order of neighboring ISIs rather than the actual values of the ISIs.[40]

NORMALIZED GSWD OCCURRENCE AND DURATION. GSWDs were detected using the offline ECoG detection algorithm described above. Total number of GSWDs and average GSWD duration were calculated and normalized to baseline values.

ASSESSMENT OF CELLULAR RESPONSES TO OPTOGENETIC STIMULATION. Action potentials were detected as described above. A custom-written LabVIEW program was used to construct light-triggered raster plots and peri–stimulus time histograms with a 5-millisecond bin width. Changes in CN neuronal firing rate upon optical stimulation were subsequently determined by calculating the total number of action potentials during light pulses divided by the total length of the pulse and compared with the baseline firing rate (calculated from the total recording time excluding the optogenetic stimulation). In the current study, we consider differences in action potential firing rate exceeding 25% as responsive.

ASSESSMENT OF IMPACT OF OPTOGENETIC CEREBELLAR OUTPUT STIMULATION ON GSWDS. The start and end of seizures were identified using the offline GSWD detection method described above. A custom-written LabVIEW program was used to assess the effectiveness of optogenetic stimulation in stopping GSWDs. Only light pulses triggered prior to the natural end of the seizure were used for analysis. The time difference between the light pulse and the end of the seizure was calculated. The seizure was considered "stopped by the optogenetic stimulation" when this time difference did not exceed 150 milliseconds. Mean power at GSWD frequency (6–9Hz) was calculated using FFT of the ECoG signal recorded during 1-second or 0.5-second (in the case of closed-loop optogenetic stimulation) time periods before and after the light pulse. Averaged responses to light pulses are represented per animal and per stimulus condition by averaging complex Morlet wavelets of 4-second windows ranging from 2 seconds before to 2 seconds after the stimulus.

ASSESSMENT OF ONSET OF OPTICAL CEREBELLAR NUCLEI STIMULATION RELATIVE TO GSWD CYCLE. The time difference between the onset of stimulation and the last spike before stimulation was calculated and divided by the median length of 1 GSWD during that episode, representing 1 cycle of 360°. The outcome was subsequently multiplied by 360. Note that the optogenetic stimuli were not initiated with a fixed delay after the occurrence of an ECoG spike; the delay depended on the visual interpretation and reaction speed of the experimenter (for manual activation of the LED) or on the closed-loop detection system for which the delay depends on the variability of the ECoG directly prior to the GSWDs (see below and van Dongen et al[41]).

CLOSED-LOOP GSWD DETECTION. The GSWD detection system has been implemented using a real-time, digital wavelet-filter setup. The analog pre-filter used for digitization has 4 functions: (1) amplification, (2) offset injection to match the signal to the input range of the analog to digital converter (ADC), (3) artifact removal by using a second-order 0.4Hz high-pass filter, and (4) antialiasing by means of a second-order 23.4Hz low-pass filter. The filter is realized using discrete components on a prototype printed circuit board (PCB). Following the PCB, the wavelet filter functionality is implemented on a TI Sitara AM335x ARM microprocessor (Texas Instruments, Dallas, TX). It first digitizes the signal from the analog filter with its integrated ADC using a sampling frequency of 100Hz. Subsequently the signal is filtered using a wavelet filter and the GSWD episode is detected using signal thresholding. Upon detection an output LED is switched on to stimulate the target area in the cerebellum. Wavelet filters have previously been successfully applied for real-time GSWD detection.[42] Here we applied a complex Morlet wavelet at 6.7Hz that resembled a GSWD. The wavelet filter was implemented as a finite impulse response filter by truncating the ideal complex Morlet wavelet as described earlier.[43] Using the 2 thresholds that are set manually during a recording session, the GSWDs are detected during a positive, high-threshold crossing and the detection is ended upon a negative, low-threshold crossing.

STATISTICAL ANALYSES. Statistical differences in firing pattern parameters between independent groups of CN neuronal recordings (eg, from *tg* mice, their wild-type littermates, GSWD-modulated and non–GSWD-modulated, before and after gabazine injection) were determined using multivariate analyses of variance (MANOVAs) with firing frequency, CV, CV2, and burst index as dependent variables and group as independent variable. When a MANOVA showed a significant result, post hoc analyses of variance (ANOVAs) were used to assess contributions of individual firing pattern parameters with Bonferroni corrected *p*-values.

Differences in coherence value between GWSD-modulated and non–GWSD-modulated cells were assessed using unpaired samples *t* tests. Cochran and Cox adjustment

for the standard error of the estimate and the Satterthwaite adjustment for the degrees of freedom were used because equality of variances was not assumed.

Differences in normalized number of GSWD episodes and their duration between traces pre- and postinjection of either muscimol, gabazine, or saline were tested by using nonparametric Friedman ANOVAs with 1 within-subjects factor (ie, time period) with 2 levels (baseline and postinjection).

Differences in mean power at 6 to 9Hz before and after a light pulse were tested using values from all individual pulses by use of repeated measures analysis of covariance (ANCOVA) with 1 within-subjects factor (ie, period) with 2 levels (before and after light pulse) and mouse number added as covariate to correct for variance in the within-subject factor explained by variance between mice. To test whether the time difference between the last ECoG spike before optogenetic stimulation and the subsequent spike deviates from the median interval between 2 ECoG spikes in "stopped seizures," a similar statistical approach was used. A repeated measures ANCOVA was used with 1 within-subject factor with 2 levels, both and ECoG spike intervals. Mouse number was again added as covariate. Because the number of seizures not terminated by the optogenetic stimulation was low, a nonparametric Friedman ANOVA was used to test the same difference.

To determine whether the phase angle of the optogenetic stimulation onset was related to the success rate of stopping GSWDs, we compared the phase angle distribution of successful attempts to that of the unsuccessful attempts. We tested for significant differences between these distributions using the nonparametric 2-sample Kuiper test.

A p-value ≤ 0.05 (α) was considered significant unless Bonferroni correction was used; in that case, a p-value of α/n was considered significant. Two-tailed testing was used for all statistical analyses and all were performed using SPSS 20.0 software (IBM, Armonk, NY). Exact information and outcomes regarding statistical testing are depicted in Tables 1 to 7.

Results

GSWD-Related CN Neuronal Activity

We first investigated whether CN neuronal activity and ECoG were correlated during spontaneous episodes of GSWDs in awake head-fixed homozygous *tg* mice (Fig 1). We found no significant differences in GSWD occurrence ($t_{24} = -0.002$, $p = 0.998$) and GSWD duration ($t_{24} = 0.195$, $p = 0.847$) between male and female *tg* mice, which is in line with data from other experimental animal models of absence epilepsy (reviewed by van Luijtelaar et al[44]). Therefore, we grouped data of both genders. GSWDs appeared simultaneously in bilateral primary motor (M1) and sensory cortices (S1) at 7.6 ± 0.6Hz with an average duration of 3.6 ± 1.4 seconds (n = 17 mice). The GSWD frequency and appearance were comparable to earlier reports of awake *tg* and other rodent models of absence epilepsy.[30,32,34,45] During these GSWDs, action potential firing of a subset of CN neurons was phase-locked to GSWDs. A typical GSWD-modulated CN neuron showed oscillatory action potential firing at GSWD frequency; repetitive firing was observed during the wave in the ECoG, whereas the spike was accompanied by a pause in CN neuronal activity. These GSWD-modulated CN neurons showed significantly increased coherence with ECoG during seizures ($p \leq 0.001$; see Table 1). In each CN type (MCN, IN, and LCN), a substantial portion of the recorded CN neurons showed GSWD-modulated firing, with the highest percentage (73%; 49 of 67 neurons) in the IN and 35% (35 of 100 neurons) and 44% (19 of 43 neurons) in the MCN and LCN, respectively. We found no statistical difference ($p = 0.512$) in the phase of modulation of neuronal firing relative to the GSWD cycle for these 3 nuclei.

To assess whether GSWD-modulated CN neurons differed from non-modulating CN neurons in baseline activity, we compared their interictal firing patterns. During interictal periods GSWD-modulated CN neurons showed a higher firing frequency and a more irregular, burstlike firing pattern compared with non-modulated neurons (p-values < 0.01), and both modulated and non-modulated groups showed a more irregular firing pattern and increased burst index compared to CN neurons recorded from wild-type littermates (p-values < 0.01; see Fig 1G, Table 1). Gaussian process regression[39] revealed that in *tg* mice interictal CN neuronal firing was correlated with the ictal firing pattern; 94% of neurons that phase-locked their activity to GSWDs could be predicted correctly, based on their interictal firing pattern (see Fig 1H). These data indicate that a large subset of neurons within each CN consistently shows seizure-modulated activity, that is, that these GSWD-modulated CN neurons are different from non-modulated neurons in basic, interictal firing patterns and that GSWD-related modulation can be predicted based on these interictal firing patterns.

Impact on GSWD Occurrence of Pharmacological Interventions That Modulate CN Action Potential Firing

CN neurons provide excitatory input to thalamic neurons[4,6,23–29] and thereby potentially contribute to the excitation–inhibition balance that sets thalamic activity patterns. Excess tonic inhibition of thalamic activity has been linked to the occurrence of absence seizures,[3,7,8] and therefore we hypothesized that a decrease in CN output in *tg* should increase the occurrence of GSWDs,

TABLE 1. CN Action Potential Firing

Tested Data	Compared Groups	*N*	*p*	*t* or *F*-value	Statistical Test
Differences in phase relation between CN modulation and GSWD cycle					
Phase relation	MCN	100	0.512	$F(2,100) = 0.674$	Watson–Williams multiple sample test
	IN	67			
	LCN	43			
Differences in CN neuronal action potential firing					
Coherence	*tg* GSWD-modulated	103	<0.001[a]	$t(195.9) = 13.35$	Independent samples *t* test
	tg non-modulated	107			
Overall	Wild type	94	<0.001[a]	$F(4,192) = 68.72$	MANOVA (Pillai's trace)
	tg GSWD-modulated interictal	103			
Firing frequency	Wild type	94	0.095	$F(1,195) = 2.81$	ANOVA (Bonferroni)
	tg GSWD-modulated interictal	103			
Coefficient of variation	Wild type	94	<0.001[a]	$F(1,195) = 58.88$	ANOVA (Bonferroni)
	tg GSWD-modulated interictal	103			
CV2	Wild type	94	<0.001[a]	$F(1,195) = 34.63$	ANOVA (Bonferroni)
	tg GSWD-modulated interictal	103			
Burst index	Wild type	94	<0.001[a]	$F(1,195) = 230.86$	ANOVA (Bonferroni)
	tg GSWD-modulated interictal	103			
Overall	Wild type	94	<0.001[a]	$F(4,196) = 16.66$	MANOVA (Pillai's trace)
	tg non-modulated interictal	107			
Firing frequency	Wild type	94	0.092	$F(1,199) = 2.86$	ANOVA (Bonferroni)
	tg non-modulated interictal	107			
Coefficient of variation	Wild type	94	<0.001[a]	$F(1,199) = 15.13$	ANOVA (Bonferroni)
	tg non-modulated interictal	107			
CV2	Wild type	94	<0.01[a]	$F(1,199) = 6.79$	ANOVA (Bonferroni)
	tg non-modulated interictal	107			
Burst index	Wild type	94	<0.001[a]	$F(1,199) = 37.99$	ANOVA (Bonferroni)
	tg non-modulated interictal	107			

TABLE 1: Continued

Tested Data	Compared Groups	*N*	*p*	*t* or *F*-value	Statistical Test
Overall	*tg* GSWD-modulated interictal	103	<0.001[a]	$F(4,205) = 17.84$	MANOVA (Pillai trace)
	tg non-modulated interictal	107			
Firing frequency	*tg* GSWD-modulated interictal	103	<0.001[a]	$F(1,208) = 16.31$	ANOVA (Bonferroni)
	tg non-modulated interictal	107			
Coefficient of variation	*tg* GSWD-modulated interictal	103	<0.01[a]	$F(1,208) = 7.12$	ANOVA (Bonferroni)
	tg non-modulated interictal	107			
CV2	*tg* GSWD-modulated interictal	103	<0.01[a]	$F(1,208) = 9.47$	ANOVA (Bonferroni)
	tg non-modulated interictal	107			
Burst index	*tg* GSWD-modulated interictal	103	<0.001[a]	$F(1,208) = 62.6$	ANOVA (Bonferroni)
	tg non-modulated interictal	107			

Corresponds to Figure 1.
[a]Statistically significant.
ANOVA = analysis of variance; CN = cerebellar nuclei; GSWD = generalized spike-and-wave discharge; IN = interposed nuclei; LCN = lateral cerebellar nuclei; MANOVA = multivariate analysis of variance; MCN = medial cerebellar nuclei.

whereas increased CN output should have the opposite effect. To test this, we locally applied (see Fig 2, Supplementary Fig) either $GABA_A$-agonist muscimol, which stopped CN neuronal action potential firing (no statistical comparison was possible due to complete cessation of action potential firing), or $GABA_A$-antagonist gabazine (SR-95531), which consistently increased the frequency ($p < 0.01$) and regularity of CN neuronal firing ($p < 0.001$; see Table 2). Upon bilateral CN injections with muscimol, the occurrence of GSWDs increased by 160 to 3,700% postinjection ($p < 0.01$; recorded for 60 minutes; peak of seizure occurrence 34.5 ± 16.5 minutes after injection; n = 10). In contrast, bilateral CN injections with gabazine significantly reduced the occurrence of GSWDs ($p < 0.05$; first seizure occurred 32.5 ± 17.4 minutes after injection; n = 10) and bilateral sham injections did not change GSWD occurrence ($p = 0.18$). The duration of GSWDs was not significantly changed following muscimol, gabazine, or saline injections in the CN (muscimol: $p = 0.21$; gabazine: $p = 0.32$; saline: $p = 0.41$). As a control, we also injected similar quantities of gabazine or muscimol into the cerebellar cortex; this had no significant effect on the GSWD occurrence ($p = 0.66$ and 0.32, respectively) or duration ($p = 0.66$ for both gabazine and muscimol injections). Thus, pharmacological manipulation of neuronal activity in the CN, but not the cerebellar cortex, is highly effective in modulating the occurrence of GSWDs in *tg* mice. Notably, we observed that muscimol and gabazine were most effective when the injections were in the IN and/or LCN (no statistical difference in impact on GSWD-occurrence after IN and/or LCN injections; $p = 0.70$; Mann–Whitney *U* test) compared to injections in the MCN ($p = 0.07$ for muscimol and $p < 0.05$ for gabazine; see Supplementary Fig, Table 3). To study whether these differences in impact of pharmacological interventions aimed at the MCN or the IN and LCN were due to a variable effect on neuronal activity, we also performed single unit recordings in the injected CN. Regardless of the injected nucleus, muscimol effectively silenced all action potential firing and gabazine consistently increased the firing frequency and the regularity of action potential firing (all *p*-values < 0.01 for firing frequency, CV, and CV2; see Table 4). These findings indicate that although effects of muscimol and gabazine on the neuronal activity were similar throughout all CN, the effect of manipulating activity in the IN and LCN seems to exert a larger impact on GSWD-occurrence in the mutants than targeting the

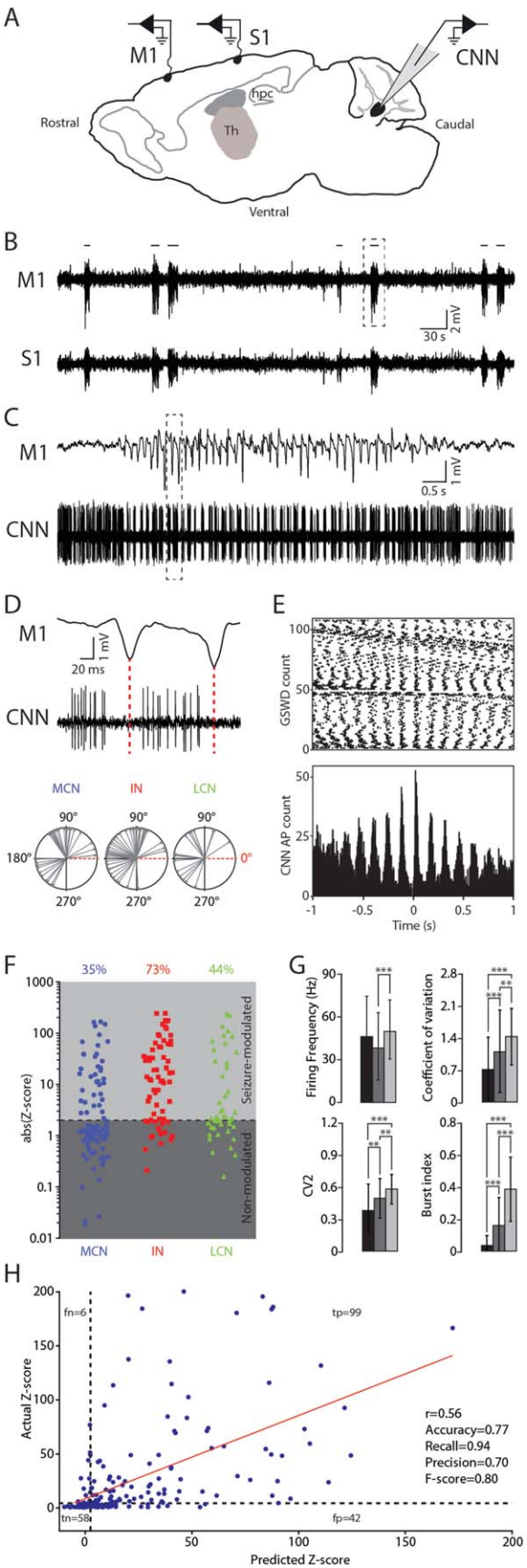

FIGURE 1

MCN. Instead, pharmacological interventions in the CN of wild-type littermates (n = 2) did not evoke GSWD-episodes (data not shown).

Although it has been shown that pharmacological interventions can have sex-specific differences in animal models of epilepsy[46] that may contribute to the variability of the current results, our ECoG recordings did not show a trend toward a sex-specific impact of CN-specific muscimol or gabazine application (see Fig 2F–H). This finding was corroborated by the finding that muscimol was equally effective in stopping CN action potential

FIGURE 1: Cerebellar nuclei (CN) neuronal action potential firing patterns are modulated during generalized spike-and-wave discharges (GSWDs). (A) Schematic of recording sites for electrocorticogram (ECoG) from primary motor (M1) and sensory (S1) cortices and extracellular single unit CN neuronal (CNN) recordings (Th = thalamus, hpc = hippocampus). (B) ECoG from M1 and S1 with GSWD episodes (horizontal lines), indicating absence seizures. (C) Zoom of M1 episode outlined in B and simultaneously recorded action potential firing of a single CN neuron. (D; top panel) Zoom of outlined M1 and CNN recording in C. Red lines align ECoG spike with pause in CNN action potential firing. Bottom panel: Compass plot of phase difference between ECoG spike and modulated CNN action potential firing. IN = interposed nuclei; LCN = lateral CN; MCN = medial CN. (E) Raster plot and accompanying peri–spike-and-wave discharge time histogram of CNN action potentials (AP) for 3 consecutive seizures (t = 0 is aligned with each ECoG spike). (F) Distribution of absolute *Z* scores of mean power at GSWD frequency as determined by fast Fourier transform for MCN, IN, and LCN. Note that none of the negative *Z* scores was below −1.96, and therefore showing absolute *Z* scores does not change the number of data points below and above the 1.96 cutoff score (corresponding to $p < 0.05$; *horizontal dashed line*). Total number of recorded neurons: MCN, n = 100; IN, n = 67; LCN, n = 43. (G) Bar plots representing firing frequency, coefficient of variation, coefficient of variation 2 (CV2), and burst index for CN neurons recorded in wild-type littermate (n = 94; black) and seizure-modulated (n = 103; light gray) and non-modulated CN neurons recorded in *tg* (n = 107; dark gray). For clarity, we truncated the negative error bars. **$p < 0.01$, ***$p < 0.001$ (multivariate analysis of variance, post hoc analyses of variance with Bonferroni correction; see Table 1). (H) Result of the Gaussian process regression to predict the *Z* score from interictal activity parameters (CV, firing frequency, log-interval entropy, and permutation entropy) represented as a confusion matrix. The prediction is characterized as being a true positive (tp) when the predicted *Z* score is >1.96 *(dotted line)* and the actual *Z* score is >1.96. A true negative (tn) is scored when both predicted and actual *Z* scores are <1.96. False positive (fp) and false negative (fn) refer to neurons that have been incorrectly predicted as GSWD modulated and GSWD non-modulated, respectively. Note that we were able to achieve a precision of 0.70 and a recall of 0.94, which means that 70% of CN neurons (n = 210) that were predicted as GSWD modulated actually were GSWD modulated, and 94% of all GSWD-modulated neurons have been identified correctly by the model. The Pearson correlation coefficient (*r*) between the predicted *Z* score and the actual *Z* score was 0.56 with $p \leq 0.05$.

firing in both male and female mice. Together, these effects indicate that in the *tg* animal model of absence epilepsy CN output forms an integral component of the neuronal networks involved in generalized epilepsy and may operate as a potent modulator of GSWD occurrence, irrespective of the gender.

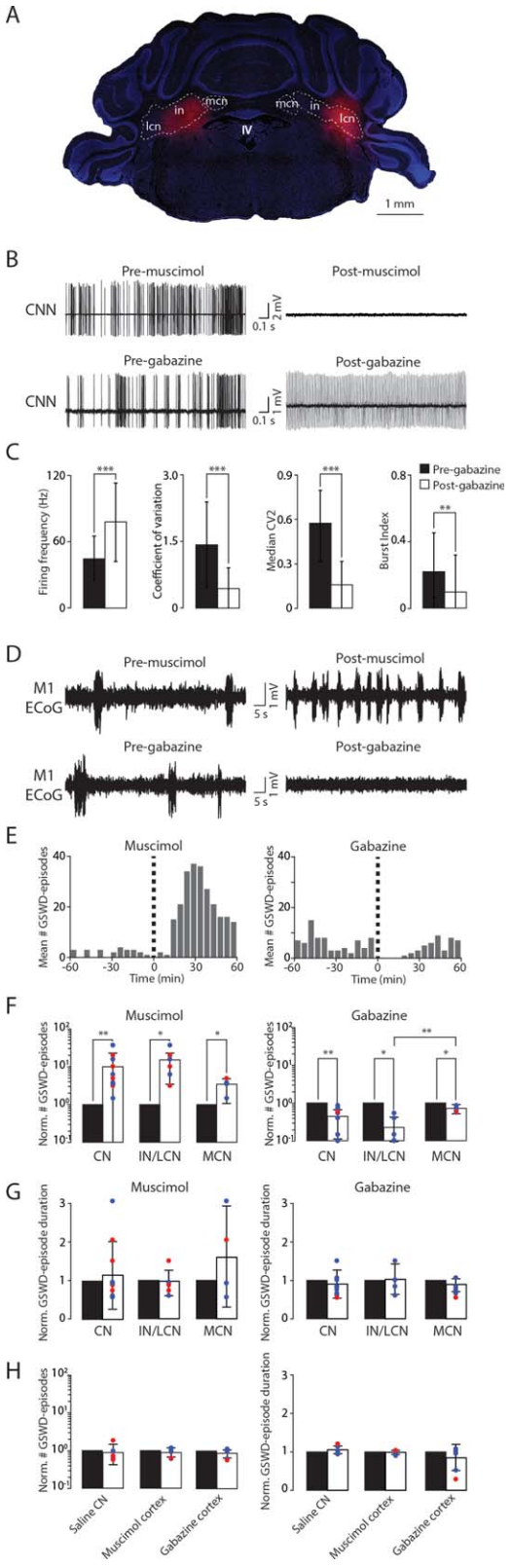

FIGURE 2

Optogenetic Stimulation of Cerebellar Nuclei

The promising impact of long-lasting pharmacological interventions at the level of the cerebellar output prompted us to explore whether short-lasting neuromodulation would be equally effective in stopping GSWDs, that is, whether disrupting oscillatory CN neuronal activity immediately stops GSWDs. To test this hypothesis, we virally expressed light-sensitive ChR2 cation channels in CN neurons (see Fig 3). The optically evoked alteration of CN neuronal firing (see below; Fig 5A) had a robust effect on GSWD occurrence, in that most if not all episodes abruptly stopped within 150 milliseconds of the onset of bilateral stimulation (n = 4; presented per mouse: 76% [male], 84% [female], 92% [female], and 100% [female] stopped) and in that the power at GSWD frequency was significantly reduced ($p < 0.001$; see Fig 3, Table 5). Moreover, unilateral optical stimulation of CN

FIGURE 2: Bimodal modulation of generalized spike-and-wave discharge (GSWD) occurrence by pharmacological manipulation of cerebellar nuclei (CN) neuronal (CNN) action potential firing. (A) Confocal image of coronal cerebellar slice with bilateral muscimol injections (blue = 4′,6-diamidino-2-phenylindole (DAPI); red = Evans blue indicating the injection sites; IN = interposed nucleus; IV = 4th ventricle; LCN = lateral CN; MCN = medial CN). (B) Examples of CNN recordings before and after bilateral muscimol (top) and gabazine (bottom) injections. (C) Bar plots for the impact of gabazine on CNN firing as quantified by the difference between pre- and postgabazine injections (n = 81 and n = 55, respectively) in firing frequency, coefficient of variation, median CV2, and burst index; **$p < 0.01$, ***$p < 0.001$ (multivariate analysis of variance, post hoc analyses of variance [ANOVAs] with Bonferroni corrections; see Table 2). (D; top) Representative electrocorticogram (ECoG) of primary motor cortex (M1) ECoG before and after muscimol injection; (bottom) representative M1 ECoG before and after gabazine injection. (E) Time course of the effects of muscimol (left) and gabazine (right) on the average number of GSWD episodes (bin size = 5 minutes). (F, G) Normalized number of seizures (F) and normalized seizure duration (G) before and after muscimol (left) and gabazine (right) injections (1 hour each) for bilateral injections in all CN (n = 10 for both gabazine and muscimol), in IN/LCN (n = 6 for muscimol and 5 for gabazine), and in MCN (n = 4 for muscimol and 5 for gabazine). Note that for quantification of the seizure duration after gabazine injection, only 9 mice are included in all CN and 4 mice in the IN/LCN group, because 1 mouse did not show any GSWDs postinjection. Blue dots indicate data recorded from male mice and red dots from female. *$p < 0.05$, **$p < 0.01$ (Friedman ANOVAs and Mann–Whitney *U* tests; see Tables 2 and 3). (H) Normalized number of GSWD episodes (left) and normalized GSWD episode duration (right) for control experiments; saline injections in the CN and muscimol and gabazine injections in superficial cerebellar cortical areas.

TABLE 2. Impact of Pharmacological Manipulations on CN Firing and GSWD Occurrence

Tested Data	Compared Groups	*N*	*p*	*F*	Statistical Test
Effects of bilateral CN gabazine injections on CNN activity					
Overall	*tg* pregabazine	81	<0.001[a]	$F(4,131) = 39.83$	MANOVA (Pillai's trace)
	tg postgabazine	55			
Firing frequency	*tg* pregabazine	81	<0.001[a]	$F(1,134) = 37.15$	ANOVA (Bonferroni)
	tg postgabazine	55			
Coefficient of variation	*tg* pregabazine	81	<0.001[a]	$F(1,134) = 61.21$	ANOVA (Bonferroni)
	tg postgabazine	55			
CV2	*tg* pregabazine	81	<0.001[a]	$F(1,134) = 117.63$	ANOVA (Bonferroni)
	tg postgabazine	55			
Burst index	*tg* pregabazine	81	<0.01[a]	$F(1,134) = 8.71$	ANOVA (Bonferroni)
	tg postgabazine	55			
Effects of pharmacological manipulations of CN neurons on GSWDs					
GSWD occurrence	*tg* presaline CN	6	0.180		Friedman's ANOVA
	tg postsaline CN				
	tg premuscimol CN	10	<0.01[a]		Friedman's ANOVA
	tg postmuscimol CN				
	tg pregabazine CN	10	<0.01[a]		Friedman's ANOVA
	tg postgabazine CN				
	tg premuscimol cortex	5	0.655		Friedman's ANOVA
	tg postmuscimol cortex				
	tg pregabazine cortex	5	0.317		Friedman's ANOVA
	tg postgabazine cortex				
GSWD duration	*tg* presaline CN	6	0.414		Friedman's ANOVA
	tg postsaline CN				
	tg premuscimol CN	10	0.206		Friedman's ANOVA
	tg postmuscimol CN				
	tg pregabazine CN	10	0.317		Friedman's ANOVA
	tg postgabazine CN				
	tg premuscimol cortex	5	0.655		Friedman's ANOVA
	tg postmuscimol cortex				
	tg pregabazine cortex	5	0.655		Friedman's ANOVA
	tg postgabazine cortex				

Corresponds to Figure 2C, F–H.
[a]Statistically significant.
ANOVA = analysis of variance; CN = cerebellar nuclei; CNN = CN neuronal; GSWD = generalized spike-and-wave discharge; MANOVA = multivariate analysis of variance.

neurons proved equally effective in stopping GSWDs in all recorded cortices, regardless of the laterality (n = 3 females; presented per mouse: 89%, 92%, and 100% stopped; power reduction: $p < 0.001$). Bilateral cerebellar stimulation was ineffective when a different wavelength (590nm) was applied (n = 3 females; presented per

TABLE 3. Impact of Local Pharmacological Manipulations on GSWD Occurrence

Tested Data	Compared Groups	*N*	*p*	Statistical Test
GSWD occurrence pre vs post	*tg* premuscimol IN/LCN	6	<0.05[a]	Friedman's ANOVA
	tg postmuscimol IN/LCN			
	tg premuscimol MCN	4	<0.05[a]	Friedman's ANOVA
	tg postmuscimol MCN			
	tg pregabazine IN/LCN	5	<0.05[a]	Friedman's ANOVA
	tg postgabazine IN/LCN			
	tg pregabazine MCN	5	<0.05[a]	Friedman's ANOVA
	tg postgabazine MCN			
GSWD occurrence medial vs lateral CN	*tg* postmuscimol IN/LCN	6	0.067	Mann–Whitney *U* test
	tg postmuscimol MCN	4		
	tg postgabazine IN/LCN	5	<0.01[a]	Mann–Whitney *U* test
	tg postgabazine MCN	5		
GSWD duration pre vs post	*tg* premuscimol IN/LCN	6	0.102	Friedman's ANOVA
	tg postmuscimol IN/LCN			
	tg premuscimol MCN	4	1.00	Friedman's ANOVA
	tg postmuscimol MCN			
	tg pregabazine IN/LCN	5	1.00	Friedman's ANOVA
	tg postgabazine IN/LCN			
	tg pregabazine MCN	5	0.180	Friedman's ANOVA
	tg postgabazine MCN			
GSWD duration medial vs lateral CN	*tg* postmuscimol IN/LCN	6	0.352	Mann–Whitney *U* test
	tg postmuscimol MCN	4		
	tg postgabazine IN/LCN	5	0.413	Mann–Whitney *U* test
	tg postgabazine MCN	5		

Corresponds to Figure 2F–G.
[a]Statistically significant.
ANOVA = analysis of variance; CN = cerebellar nuclei; GSWD = generalized spike-and-wave discharge; IN = interposed nuclei; LCN = lateral cerebellar nuclei; MCN = medial cerebellar nuclei.

mouse: 0%, 0%, and 5% stopped; power reduction: $p = 0.37$) or when the optical fiber was placed outside the CN region (n = 3 females; presented per mouse: 0%, 5%, and 8% stopped; power reduction: $p = 0.28$).

The type of seizure detection and on-demand stimulation described above renders the procedure conceptually unsuitable for clinical implementation in that it would require constant online evaluation and decision making by medics.[47] Therefore, we developed a brain–machine interface (BMI) approach by engineering a closed-loop system for online detection of GSWDs and subsequent optogenetic stimulation.[41] Using offline analysis, we optimized the performance of a wavelet-based GSWD detection filter up to an accuracy of 96.5% and a median latency of 424 milliseconds. When applied online, this on-demand, closed-loop stimulation proved efficient in detecting and stopping GSWDs; bilateral optical stimulation of ChR2-expressing CN neurons stopped 93.4% of GSWDs and unilateral stimulation stopped 91.8% of GSWDs, which is also represented by the GSWD frequency power reduction (n = 3 female; $p < 0.001$; see Fig 3E, F, Table 5). Together, these data highlight that in a clinically applicable BMI setting single pulse stimulation of CN

TABLE 4. Impact of Local Pharmacological Manipulations on CN Spiking Activity

Tested Data	Compared Groups	*N*	*p*	*F*-value	Statistical Test
Overall	*tg* pregabazine IN/LCN	40	<0.001[a]	$F(4,62) = 12.41$	MANOVA (Pillai's trace)
	tg postgabazine IN/LCN	27			
Firing frequency	*tg* pregabazine IN/LCN	40	<0.01[a]	$F(1,65) = 8.80$	ANOVA (Bonferroni)
	tg postgabazine IN/LCN	27			
Coefficient of variation	*tg* pregabazine IN/LCN	40	<0.001[a]	$F(1,65) = 23.18$	ANOVA (Bonferroni)
	tg postgabazine IN/LCN	27			
CV2	*tg* pregabazine IN/LCN	40	<0.001[a]	$F(1,65) = 25.13$	ANOVA (Bonferroni)
	tg postgabazine IN/LCN	27			
Burst index	*tg* pregabazine IN/LCN	40	<0.01[a]	$F(1,65) = 10.22$	ANOVA (Bonferroni)
	tg postgabazine IN/LCN	27			
Overall	*tg* pregabazine MCN	41	<0.001[a]	$F(4,64) = 40.55$	MANOVA (Pillai's trace)
	tg postgabazine MCN	28			
Firing frequency	*tg* pregabazine MCN	41	<0.001[a]	$F(1,67) = 37.53$	ANOVA (Bonferroni)
	tg postgabazine MCN	28			
Coefficient of variation	*tg* pregabazine MCN	41	<0.001[a]	$F(1,67) = 60.04$	ANOVA (Bonferroni)
	tg postgabazine MCN	28			
CV2	*tg* pregabazine MCN	41	<0.001[a]	$F(1,67) = 153.36$	ANOVA (Bonferroni)
	tg postgabazine MCN	28			
Burst index	*tg* pregabazine MCN	41	0.614	$F(1,67) = 0.61$	ANOVA (Bonferroni)
	tg postgabazine MCN	28			
Overall	*tg* pregabazine IN/LCN	40	<0.001[a]	$F(4,76) = 6.28$	MANOVA (Pillai's trace)
	tg pregabazine MCN	41			
Firing frequency	*tg* pregabazine IN/LCN	40	0.438	$F(4,79) = 0.61$	ANOVA (Bonferroni)
	tg pregabazine MCN	41			
Coefficient of variation	*tg* pregabazine IN/LCN	40	0.037	$F(4,79) = 4.51$	ANOVA (Bonferroni)
	tg pregabazine MCN	41			
CV2	*tg* pregabazine IN/LCN	40	0.494	$F(4,79) = 0.47$	ANOVA (Bonferroni)
	tg pregabazine MCN	41			
Burst index	*tg* pregabazine IN/LCN	40	<0.001[a]	$F(4,79) = 13.53$	ANOVA (Bonferroni)
	tg pregabazine MCN	41			
Overall	*tg* postgabazine IN/LCN	27	<0.001[a]	$F(4,50) = 4.29$	MANOVA (Pillai's trace)
	tg postgabazine MCN	28			
Firing frequency	*tg* postgabazine IN/LCN	27	0.344	$F(4,53) = 0.91$	ANOVA (Bonferroni)
	tg postgabazine MCN	28			
Coefficient of variation	*tg* postgabazine IN/LCN	27	≤0.001[a]	$F(4,53) = 13.55$	ANOVA (Bonferroni)
	tg postgabazine MCN	28			
CV2	*tg* postgabazine IN/LCN	27	<0.01[a]	$F(4,53) = 10.16$	ANOVA (Bonferroni)
	tg postgabazine MCN	28			
Burst index	*tg* postgabazine IN/LCN	27	0.801	$F(4,53) = 0.64$	ANOVA (Bonferroni)
	tg postgabazine MCN	28			

[a]Statistically significant.
ANOVA = analysis of variance; IN = interposed nuclei; LCN = lateral cerebellar nuclei; MANOVA = multivariate analysis of variance; MCN = medial cerebellar nuclei.

neurons suffices to stop GSWDs and that unilateral stimulation is sufficiently powerful to disrupt bilateral thalamocortical oscillations.

Key Findings Are Replicated in an Unrelated Mouse Model of Absence Epilepsy

To exclude the possibility that our current findings in *tg* are unique to their pathophysiology,[30,48,49] we repeated key experiments in *C3H/HeOuJ*, an inbred strain with an absence epilepsy phenotype[33] that is unrelated to *tg*. Extracellular recordings in awake ECoG-monitored *C3H/HeOuJ* mice confirmed that a smaller but substantial portion (35%) of CN neurons showed phase-locked action potential firing and significant coherence with ECoG ($p < 0.001$) during GSWDs and that this oscillatory firing was more irregular than their interictal firing pattern ($p < 0.001$; Fig 4, Table 6). Similar to *tg* mutants (see Fig 2), *C3H/HeOuJ* mice showed significantly more seizures following local muscimol injections into CN ($p < 0.05$; see Fig 4, Table 6). Moreover, also in *C3H/HeOuJ* mice optogenetic stimulation reliably stopped GSWD episodes (n = 3; presented per mouse: 82%, 87%, and 91% stopped) and both bilateral and unilateral stimuli significantly reduced power at GSWD frequency ($p < 0.01$ and $p < 0.001$, respectively); the closed-loop detection and intervention system reduced the GSWD frequency power ($p < 0.001$ for bilateral and $p < 0.05$ for unilateral stimulation); and neither optical stimulation at 590nm nor stimulation outside of CN significantly reduced the GSWD frequency power ($p = 0.43$ and $p = 0.81$, respectively). Thus, the main findings from CN treatment of absence seizures in *tg* could be replicated in *C3H/HeOuJ* mutants.

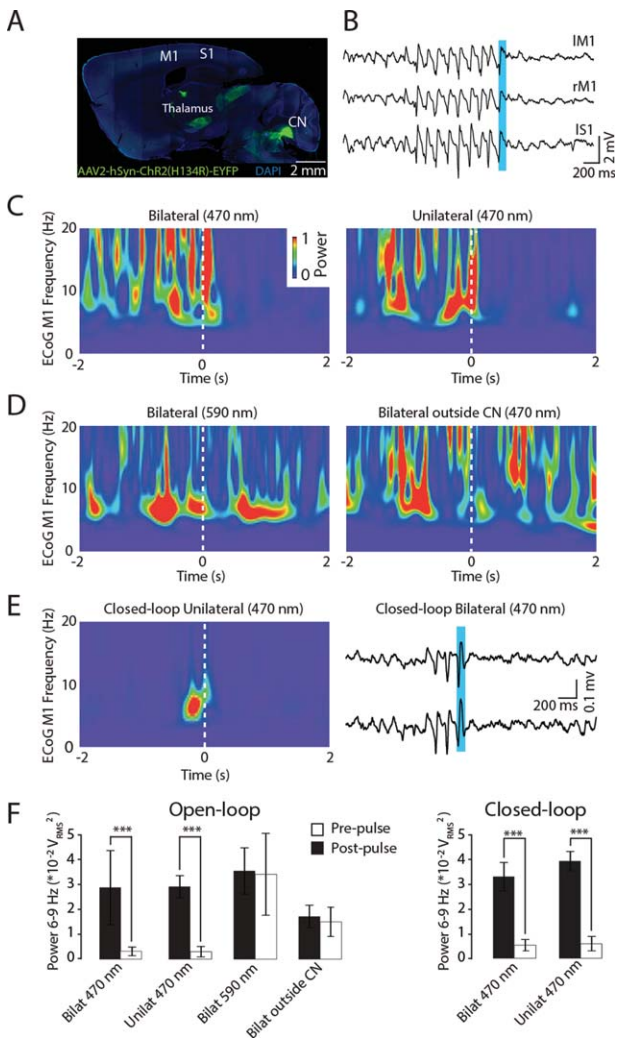

FIGURE 3

Optogenetic Stimulation of Presumptively Excitatory CN Neurons Affects GSWDs

To investigate the mechanism underlying the potent interruption of GSWDs by optogenetic stimulation of CN in *tg* and *C3H/HeOuJ*, we quantified the responses of CN neurons to bilateral optical stimulation. In *C3H/HeOuJ* and *tg* injected with AAV2-hSyn-ChR2(H134R)-EYFP, 33 of 50 responsive cells (66%) showed increased action potential firing, whereas 17 (34%) showed decreased firing (see Fig 5A). A further 16 recorded neurons showed no response to optical stimulation. This variety of responses is in line with the properties of the construct that was used to transfect CN neurons with ChR2. Because human synapsin (hSyn) is not specific to a certain type of neuron,[50] both excitatory and inhibitory CN neurons expressed ChR2. Excitatory responses can

FIGURE 3: Optogenetic stimulation of cerebellar nuclei reliably stops generalized spike-and-wave discharges (GSWDs). (A) Confocal image of sagittal brain section showing channelrhodopsin-2 (ChR2) expression in cerebellar nuclei (CN) with projections to the thalamus (M1, S1 represent primary motor and sensory cortex, respectively). (B) Representative electrocorticogram (ECoG) of bilateral M1 (left M1 [lM1], right [rM1], and left S1 [lS1] recording), which exemplifies how bilateral optogenetic stimulation (470nm light pulse of 100 milliseconds indicated by the *vertical blue bar*) stops GSWDs in all recorded cortices. (C) Mean ECoG wavelet spectrogram of contralateral M1 for all bilateral (n = 25; left panel) and unilateral stimuli (n = 11; right panel) presented to a single mouse at 470nm. (D) As in C for (left) 590nm stimuli (n = 36) and (right) stimulation at 470nm outside of CN (n = 18). (E; right) Typical example of the effect of bilateral closed-loop stimulation on GSWD recorded in contralateral M1 and S1 and (left) mean ECoG wavelet spectrogram of all unilateral stimuli (n = 44) presented to 1 mouse. (F) ECoG theta-band power before and after open-loop (bilateral: 3 females, 1 male, n = 178; unilateral: 3 female, n = 43) stimulations with the wrong wavelength (590nm; 3 females, n = 107) and stimulations outside the CN (3 females; n = 185) as well as the responses to closed-loop stimulation at 470nm in the CN (bilateral: 3 females, n = 227; unilateral: 3 females, n = 49). ***$p < 0.001$ (repeated measures analysis of covariance; see Table 5).

TABLE 5. Effect of Optogenetic CN Stimulation on GSWD-Related Power

Tested Data	Compared Groups	*N*	*p*	*F*-value	Statistical Test
Open-loop bilateral 470nm	*tg* prestimulation	178	<0.001[a]	$F(1,176) = 74.87$	Repeated measures ANCOVA
	tg poststimulation				
Open-loop unilateral 470nm	*tg* prestimulation	43	<0.001[a]	$F(1,41) = 35.25$	Repeated measures ANCOVA
	tg poststimulation				
590nm	*tg* prestimulation	107	0.367	$F(1,65) = 0.82$	Repeated measures ANCOVA
	tg poststimulation				
470nm outside CN	*tg* prestimulation	185	0.283	$F(1,65) = 1.16$	Repeated measures ANCOVA
	tg poststimulation				
Closed-loop bilateral 470nm	*tg* prestimulation	227	<0.001[a]	$F(1,65) = 456.3$	Repeated measures ANCOVA
	tg poststimulation				
Closed-loop unilateral 470nm	*tg* prestimulation	49	<0.001[a]	$F(1,65) = 97.58$	Repeated measures ANCOVA
	tg poststimulation				

Corresponds to Figure 3.
[a]Statistically significant.
ANCOVA = analysis of covariance; CN = cerebellar nuclei; GSWD = generalized spike-and-wave discharge.

be recorded from neurons that express ChR2, and inhibitory responses can be recorded from neurons that do not express ChR2 but that receive input from ChR2-positive inhibitory neurons, but neurons devoid of ChR2 expression either in their membrane or synaptic afferents will not show any response.

Next, we questioned to what extent the impact of optogenetic stimulation of CN neuronal action potential firing depends on the phase of the thalamocortical oscillations, that is, to what extent the disruption of GSWD-modulated CN firing was evoked during cortical excitation (the ECoG spike) and/or cortical inhibition (the ECoG wave).[51] Because we did not design our stimulation protocol to be activated with a fixed delay relative to the GSWDs, we could answer this question by comparing the phase values of the onset of effective stimuli relative to the spike-and-wave cycle in M1 and S1 cortices with those of ineffective stimuli (see Fig 5). For both M1 and S1, success rates were lowest when the stimulus was applied up to 60° before the peak of a spike (ie, 300°–360° in Fig 5C lower panels), but the overall differences of these distributions did not reach statistical significance (M1: $p = 0.13$; S1: $p = 0.29$). However, effective stimuli evoked a significant shortening ($p < 0.01$) of the interval between the last 2 ECoG spikes, which is indicative of an excitatory effect on cortical activity (Fig. 5D),[51] and the timing of the last ECoG spike could be predicted by the time of the stimulus onset relative to the spike-and-wave cycle ($p < 0.001$; see Fig 5E, Table 7). Together, our combined electrophysiological and optogenetic data indicate that optogenetic CN stimulation is most effective when applied during the "wave" of the GSWD, during which cortical neurons are normally silent.

Discussion

In this study, we show that in 2 unrelated mouse models of absence epilepsy the activity of CN neurons can be utilized to modulate the occurrence of GSWDs. We provide evidence that pharmacological interventions at the level of CN can exert slow, but long-term, effects and that optogenetic stimulation of CN neurons can exert fast, short-term control. The different dynamics of these experimental approaches, with converging outcomes, align with the hypothesis that CN neurons can control the balance of excitation and inhibition in the thalamus, thereby resetting the oscillatory activity in thalamocortical loops. In both *tg* and *C3H/HeOuJ* strains of mice, a substantial subset of CN neurons showed phase-locked action potential firing during GSWDs, which is in line with a previous study of oscillating cerebellar activity during GSWDs in WAG/Rij and F344/BN rats.[32] We observed that 35% of neuronal recordings in the MCN showed GSWD-modulated patterns, whereas the portions

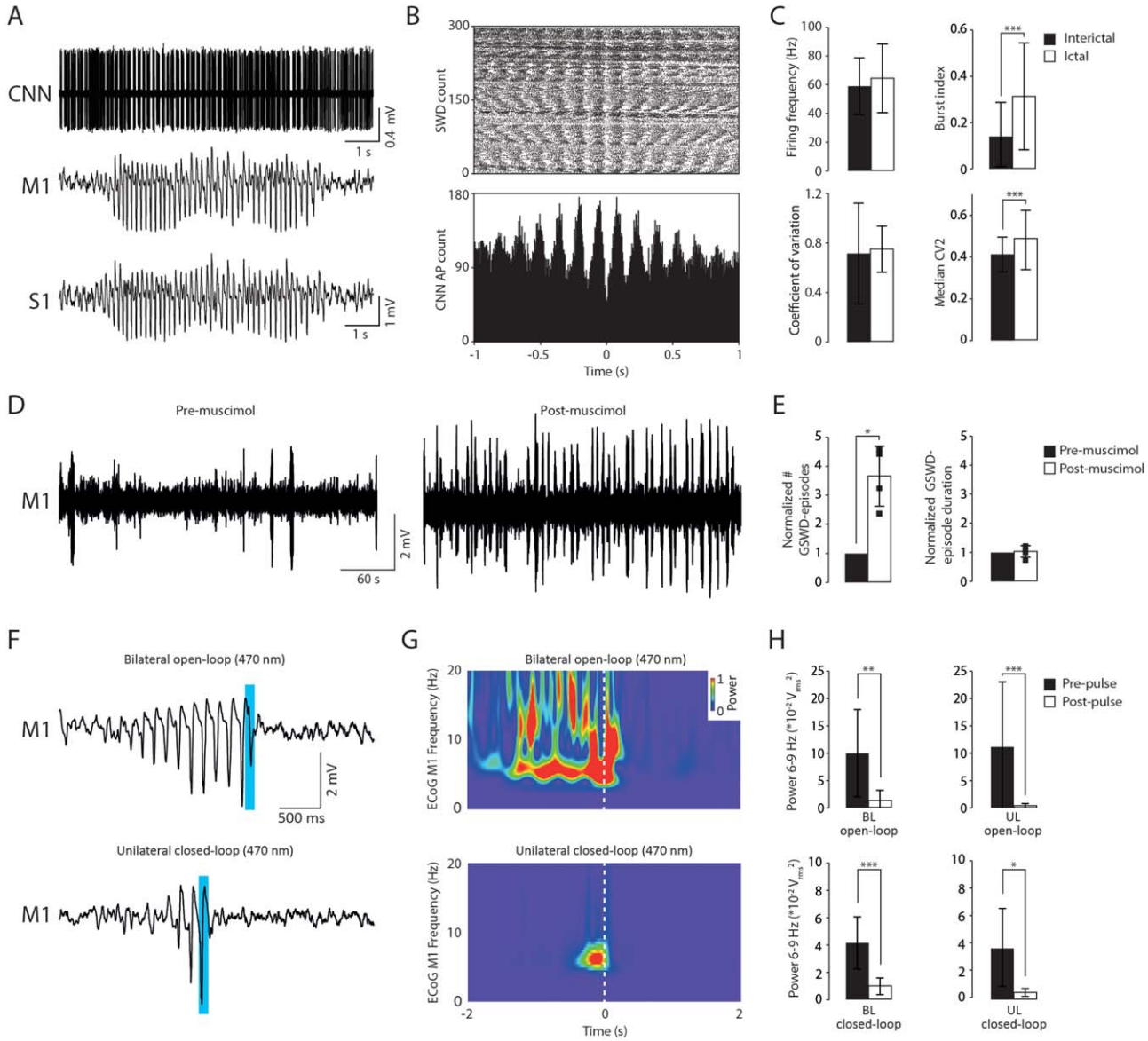

FIGURE 4: Modulation of phase-locked cerebellar nuclei (CN) neuronal (CNN) activity stops generalized spike-and-wave discharges (GSWDs) in *C3H/HeOuJ mice*. (A) Simultaneously recorded primary motor (M1) and sensory (S1) cortex electrocorticograms (ECoGs) and CNN activity. (B) Raster plot and peri–stimulus time histogram of single CNN activity (t = 0 indicates each ECoG spike). AP = action potential; SWD = spike-and-wave discharge. (C) Summary bar plots representing the mean differences in firing pattern parameters between interictal and ictal periods (n = 28). ***$p < 0.001$ (repeated measures analysis of variance [ANOVA] with Bonferroni corrections; see Table 6). (D) Representative M1 ECoG before and after muscimol injection and (E) corresponding normalized seizure occurrence and duration. *$p < 0.05$ (Friedman ANOVA; see Table 6). (F–H) Open-loop (top) and closed-loop (bottom) optogenetic stimulation stops GSWDs as shown by: (F) typical example trace; (G) ECoG wavelet spectrogram averaged over all bilateral open-loop (n = 11; top panel) stimuli in a single mouse and over all unilateral closed-loop stimuli (n = 18; bottom panel) in another mouse; and (H) ECoG theta-band power before and after optical stimulation for bilateral open-loop stimuli (n = 3 mice, n = 19 stimulations; top left panel), unilateral open-loop stimuli (n = 3 mice, n = 19 stimulations), bilateral closed- loop stimuli (n = 3 mice, n = 46 stimulations), and unilateral closed-loop stimuli (n = 3 mice, n = 30 stimulations). *$p < 0.05$, **$p < 0.01$ ***$p < 0.001$ (repeated measures ANCOVA; see Table 6).

of GSWD-modulated neurons in the IN and LCN were higher (73% and 44%, respectively). Except for an anatomical evaluation of the local density of large and small soma-diameter CN neurons in the mouse brain[52] and computational studies on the clustering analysis of CN neuronal action potential firing in *tg*,[53,54] few experimental data are available that allow us to unequivocally pinpoint the type(s) of CN neurons responsible for modification of GSWD activity. With respect to the extracellular recordings, we presumably recorded mostly

TABLE 6. Neuronal Firing and Effect of CN Manipulations on GSWD Occurrence

Tested Data	Compared Groups	*N*	*p*	*t* or *F*-value	Statistical Test
Differences in CN neuronal action potential firing					
Coherence	*C3H/HeOuJ* GSWD-modulated	28	<0.001[a]	$t(66.6) = 5.92$	Independent samples *t* test
	C3H/HeOuJ non-modulated	51			
Firing frequency	*C3H/HeOuJ* GSWD-modulated ictal	28	0.138	$F(1,27) = 2.34$	Repeated measures ANOVA (Bonferroni)
	C3H/HeOuJ GSWD-modulated interictal				
Coefficient of variation	*C3H/HeOuJ* GSWD-modulated ictal	28	0.708	$F(1,27) = 0.14$	Repeated measures ANOVA (Bonferroni)
	C3H/HeOuJ GSWD-modulated interictal				
CV2	*C3H/HeOuJ* GSWD-modulated ictal	28	<0.001[a]	$F(1,27) = 21.35$	Repeated measures ANOVA (Bonferroni)
	C3H/HeOuJ GSWD-modulated interictal				
Burst index	*C3H/HeOuJ* GSWD-modulated ictal	28	<0.001[a]	$F(1,27) = 15.64$	Repeated measures ANOVA (Bonferroni)
	C3H/HeOuJ GSWD-modulated interictal				
Effects of pharmacological manipulations of CN neurons on GSWDs					
GSWD occurrence	*C3H/HeOuJ* premuscimol	4	<0.05[a]		Friedman's ANOVA
	C3H/HeOuJ postmuscimol				
GSWD duration	*C3H/HeOuJ* premuscimol	4	0.317		Friedman's ANOVA
	C3H/HeOuJ postmuscimol				
Effects of optogenetic CN stimulation on GSWD-related power					
Open-loop bilateral 470nm	*C3H/HeOuJ* prestimulation	37	<0.01[a]	$F(1,35) = 8.17$	Repeated measures ANCOVA
	C3H/HeOuJ poststimulation				
Open-loop unilateral 470nm	*C3H/HeOuJ* prestimulation	19	<0.001[a]	$F(1,17) = 20.32$	Repeated measures ANCOVA
	C3H/HeOuJ poststimulation				
590nm in CN	*C3H/HeOuJ* prestimulation	47	0.809	$F(1,45) = 0.06$	Repeated measures ANCOVA
	C3H/HeOuJ poststimulation				

TABLE 6: Continued

Tested Data	Compared Groups	*N*	*p*	*t* or *F*-value	Statistical Test
470nm outside CN	*C3H/HeOuJ* prestimulation	56	0.425	$F(1,54) = 0.65$	Repeated measures ANCOVA
	C3H/HeOuJ poststimulation				
Closed-loop bilateral 470nm	*C3H/HeOuJ* prestimulation	46	<0.001[a]	$F(1,44) = 14.20$	Repeated measures ANCOVA
	C3H/HeOuJ poststimulation				
Closed-loop unilateral 470nm	*C3H/HeOuJ* prestimulation	30	<0.05[a]	$F(1,28) = 4.60$	Repeated measures ANCOVA
	C3H/HeOuJ poststimulation				

Corresponds to Figure 4.
[a]Statistically significant.
ANCOVA = analysis of covariance; ANOVA = analysis of variance; CN = cerebellar nuclei; GSWD = generalized spike-and-wave discharge.

from CN neurons with a large soma-diameter,[55] which incorporates mainly excitatory glutamatergic neurons,[56] but in the MCN also inhibitory glycinergic projection neurons.[57] Interestingly, GSWD-modulated CN neurons also showed characteristic firing patterns during the periods in between seizures. During these interictal periods, they fired at higher frequencies with a more irregular and burstlike pattern than the CN neurons that did not comodulate with GSWDs. Thus, the interictal firing pattern of CN neurons in *tg* and *C3H/HeOuJ* mice appears to reliably predict whether these cells will show oscillations phase-locked to GSWDs during seizures.

Pharmacological manipulation of neuronal activity in the cerebellum proved effective when the injections of muscimol or gabazine were aimed at the CN, but not when the cerebellar cortex was targeted.

We found that gabazine application was effective in reducing GSWD occurrence in all CN, with the most pronounced effects in IN and LCN. Along the same line, muscimol injections in IN and LCN evoked the biggest increase in GSWD occurrence. Effects of MCN injections were smaller but still significant. Because we know little about the density of individual types of neurons throughout the murine MCN, IN, and LCN,[52,56] and considering the similarity in effects of gabazine and muscimol on neuronal activity in these nuclei, we cannot draw a firm conclusion about a potentially differential effect of either gabazine or muscimol on the respective nuclei. These data raise the possibility that the difference in impact on GSWD occurrence between manipulation of MCN versus that of IN and LCN does not reflect a difference in intrinsic activity, but rather a difference in their efferent projections to the brainstem, midbrain, and thalamus.[24] Although all CN have been shown to project to a wide range of thalamic subnuclei, such as the ventrolateral, ventromedian, centrolateral, centromedian, and parafascicular nuclei,[24,58] and thereby connect to a variety of thalamocortical networks, the impact of IN and LCN has been shown to focus on the primary motor cortex, whereas MCN impact more diffusely on thalamocortical networks.[59]

CN axons that project to the thalamus have been shown to originate from glutamatergic neurons, which synapse predominantly perisomatically and evoke substantial excitatory responses.[4,6,23–29] Upon CN injections with muscimol, we must in effect have substantially reduced the level of excitation of thalamic neurons and thereby disturbed the balance of inhibition and excitation in thalamocortical networks in favor of inhibition. One of the main consequences of hyperpolarizing the membrane potential of thalamic neurons through this inhibition is activation of hyperpolarization-activated depolarizing cation currents (I_h) and $Ca_V3.1$ (T-type) Ca^{2+} channel currents, which typically results in the burstlike action potential firing that can drive GSWDs in thalamocortical networks.[7,8,60,61] Moreover, in *tg* thalamic relay neurons show increased T-type Ca^{2+} channel currents,[62] which probably act synergistically with the decreased excitation following muscimol treatment, likely further increasing GSWD occurrence. In contrast, when

we applied gabazine to CN, the balance of inhibition and excitation in the thalamocortical networks probably shifted toward excitation and thereby may have prevented the activation of I_h and T-type Ca^{2+} channel currents, reducing the occurrence of burst firing and GSWDs. The successful application of short periods of optogenetic excitation of CN neurons not only confirmed the deoscillating impact of gabazine, but further refined it by revealing that GSWDs can be most efficiently stopped when the interval between ECoG spikes, that is, wavelength of the oscillations, is instantly shortened and thereby reset. Given the relatively low success rate of optogenetic stimulation in the period just preceding the "spike" state of the GSWDs, which reflects the excitation state of the thalamocortical relay neurons, it is parsimonious to explain the effective resetting through optimal interference during the inhibitory or "wave" state of the GSWD.[51] This explanation centered on the resetting hypothesis argues against the possibility that GSWDs were terminated by optogenetic activation of the CN neurons that were inhibited. Regardless of the net effect of CN stimulation on thalamocortical networks, the current approach proved equally effective when applied bilateral or unilateral. Most likely, instantly resetting the balance of excitation and inhibition in thalamocortical relay neurons on one side of the brain will also engage the other side through combined ipsi- and contralateral projections from the CN to the thalamus and through interthalamic and intercortical connections.[6,24,63]

It remains to be established to what extent the current findings for absence epilepsy can help to treat epileptic patients suffering from other types of seizures. Our findings on the impact of optogenetic manipulation of CN firing patterns on GSWD occurrence seem to support the (pre)-clinical studies that apply deep brain stimulation (DBS)[64,65] in the CN may be an option to treat epilepsy patients. So far, only 3 clinical studies applying electrical DBS to the CN have been reported, which is in contrast to the dozens of studies performed to investigate the therapeutic use of cerebellar surface stimulation (as reviewed by Krauss and Koubeissi[66]). Although

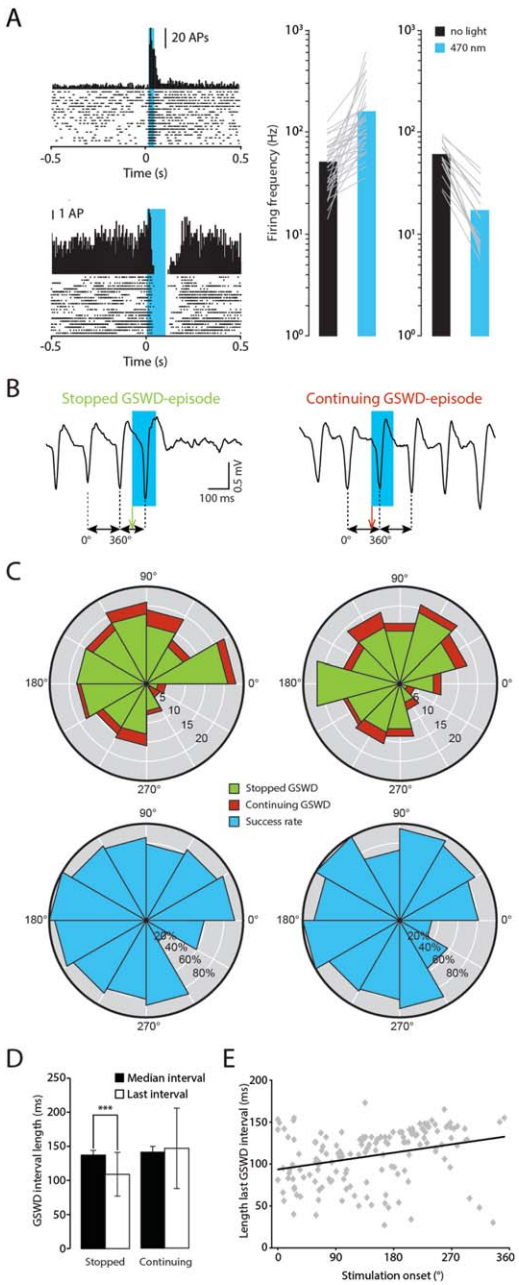

FIGURE 5

FIGURE 5: Excitatory impact of optical cerebellar nuclei (CN) stimulation on cortical activity stops generalized spike-and-wave discharge (GSWD) episodes. (A; left panels) Peri–stimulus time histogram and raster plot indicating increased (top) or decreased (bottom) action potential (AP) firing for individual CN neurons evoked by 470nm light pulses *(blue bars)*. Right panels: Scatterplots represent the individual changes in CN neuronal firing following optical stimulation: (left) increased firing (n = 33); (right) decreased firing (n = 17). Black and blue bars indicate mean firing frequency when the 470nm light-emitting diode was turned off or on, respectively. (B) Examples of stopped (left) and continuing (right) GSWD episodes upon optogenetic stimulation. Black horizontal arrows represent the median time interval between electrocorticogram (ECoG) spikes, which correspond to 1 cycle of cortical oscillation, here represented as 360°. Green and red vertical arrows represent the onset of the light stimulus. (C) Rose plots of the start of successful and unsuccessful optical stimulation in the 360° GSWD cycle for both primary motor cortex (left) and primary sensory cortex (right). (D) Comparison between the median and the last interval (between the last 2 ECoG spikes) for stopped and continuing GSWD episodes. ***$p < 0.001$ (repeated measures ANCOVA; see Table 7). (E) Scatterplot representing the predictability of the stimulus-related time interval between GSWDs by the phase of stimulation onset. $p < 0.001$ (linear regression analysis; see Table 7).

TABLE 7. Effect of Optogenetic CN Stimulation on ECoG

Tested Data	Compared Groups	*N*	*p*	*F* or *t*-value	Statistical Test
Effects of optogenetic CN stimulation on the time interval between ECoG spikes in M1					
Stopped seizures	Median interval	153	<0.001[a]	$F(1,151) = 99.80$	Repeated measures ANCOVA
	Stimulus-related interval				
Continuing seizures	Median interval	25	0.088		Friedman's ANOVA
	Stimulus-related interval				
Effects of optogenetic CN stimulation on the time interval between ECoG spikes in S1					
Stopped seizures	Median interval	153	<0.01[a]	$F(1,151) = 7.22$	Repeated measures ANCOVA
	Stimulus-related interval				
Continuing seizures	Median interval	25	0.201		Friedman's ANOVA
	Stimulus-related interval				
Predictability of stimulus-related time interval by phase of stimulation onset					
Stopped seizures		153	<0.001[a]	$t(152) = 3.87$	Linear regression

Corresponds to Figure 5.
[a]Statistically significant.
ANCOVA = analysis of covariance; ANOVA = analysis of variance; CN = cerebellar nuclei; ECoG = electrocorticogram.

initially promising, the clinical studies on the effects of cerebellar surface stimulation reported inconsistent results,[12–21] which may partially be due to suboptimal placement of electrodes. Unlike the current results, which show a regional preference for the effect of lateral CN stimulation on GSWD occurrence, it was recently shown that manipulating Purkinje cells in the medial cerebellum is most effective in controlling kainate-induced temporal lobe epilepsy.[67] So far, the studies that applied DBS at the level of CN in an uncontrolled fashion report highly effective decreases in the level of seizures (corresponding to class IC and IIIA of the Engel scale[68]) in a low number of patients characterized with various types of epilepsy.[69–71] Apart from the coherence in location of stimulation (laterally located nucleus dentatus), these studies used a wide variety in CN stimulus regimes, ranging from 3 minutes per day to continuous electrical stimulation for 12 to 14 hours per day. It appears that high-frequency stimulation (>50Hz), but not low-frequency stimulation (1–40Hz), is most effective when applied to the cerebellar dentate nucleus. In the present study, we found that the increase in CN neuronal action potential firing frequency upon optogenetic stimulation was highly variable (see Fig 4), and thus our current results do not provide any ground for a conclusion on whether low- or high-frequency stimulation would be advantageous to stop GSWD episodes. However, our results do provide sufficient data to conclude that the temporal precision determines the level of efficiency, for example, by stimulating with short pulses as soon as an epileptic event starts to occur and if possible in a proper temporal relation with respect to the inhibitory wave of the GSWDs.

Because absence epilepsy is a commonly prevalent but in essence a benign form of generalized epilepsy,[1] DBS will not very likely be considered as a serious option. However, patients diagnosed with other forms of epilepsy who do not benefit sufficiently from medication may be eligible for (cerebellar) DBS.[47] Currently, the options for applying DBS are limited; only the anterior thalamic nucleus is currently described in the US Food and Drug Administration guidelines to treat intractable epilepsy, and although promising, the outcome is limited and can result in cognitive and emotional problems.[72,73] Given the powerful impact of CN stimulation on thalamocortical activity that is shown in the present study, we hypothesize that CN stimulation may also exert very positive effects in these other, more severe kinds of epilepsies.

Acknowledgment

Support was provided by the Netherlands Organization for Scientific Research (NWO)-ALW, MAGW, ZON-MW

(A.M.J.M.v.d.M, C.I.D.Z., F.E.H.); an EU "EUROHEADPAIN" grant (602633; A.M.J.M.v.d.M); LUMC Fellowship, Marie Curie Career Integration grant and CURE SUDEP research award (E.A.T.); the Center for Medical Systems Biology in the framework of the Netherlands Genomics Initiative (A.M.J.M.v.d.M.); Neuro-Basic, European Research Counsel (ERC)-Advanced, and ERC-POC (C.I.D.Z.); and NWO-VENI, NWO-VIDI, and EUR-Fellowship (F.E.H.).

We thank Dr K. Deisseroth for providing the AAV-hSyn-ChR2(H134R)-EYFP construct and Dr T. J. Ruigrok, Dr L. Bosman, Dr P. Holland, Dr. K. Voges, R. Seepers, E. Haasdijk, E. Goedknegt, M. Rutteman, D. Groeneweg, and P. Plak for technical assistance and/or constructive discussions.

Authorship

L.K., O.H.J.E.R., and F.E.H. conceived and designed the study and performed all recordings; L.K., O.H.J.E.R., P.A., J.K.S., E.A.T., C.S., N.D., B.H.J.W., M.N., V.S., C.I.D.Z., and F.E.H. designed the analyses; L.K., O.H.J.E.R., P.A., J.K.S., and F.E.H. performed the analyses; M.N.v.D., A.K., C.S., and W.A.S. designed the closed-loop circuit; W.A.S, V.S., A.M.J.M.v.d.M., C.I.D.Z., and F.E.H contributed financial support; L.K., O.H.J.E.R., P.A., E.A.T, V.S., A.M.J.M.v.d.M., C.I.D.Z., and F.E.H. cowrote the manuscript. L.K. and O.H.J.E.R. contributed equally. C.I.D.Z. and F.E.H. contributed equally and are co-senior authors.

Potential Conflicts of Interest

Nothing to report.

References

1. Berg AT, Berkovic SF, Brodie MJ, et al. Revised terminology and concepts for organization of seizures and epilepsies: report of the ILAE Commission on Classification and Terminology, 2005–2009. Epilepsia 2010;51:676–685.
2. Jallon P, Loiseau P, Loiseau J. Newly diagnosed unprovoked epileptic seizures: presentation at diagnosis in CAROLE study. Coordination Active du Reseau Observatoire Longitudinal de l' Epilepsie. Epilepsia 2001;42:464–475.
3. Snead OC III. Basic mechanisms of generalized absence seizures. Ann Neurol 1995;37:146–157.
4. Norden AD, Blumenfeld H. The role of subcortical structures in epilepsy. Epilepsy Behav 2002;3:219–231.
5. Paz JT, Bryant AS, Peng K, et al. A new mode of corticothalamic transmission revealed in the Gria4(-/-) model of absence epilepsy. Nat Neurosci 2011;14:1167–1173.
6. Jones EG. The thalamus. 2nd ed. New York, NY: Cambridge University Press, 2007.
7. Blumenfeld H, McCormick DA. Corticothalamic inputs control the pattern of activity generated in thalamocortical networks. J Neurosci 2000;20:5153–5162.
8. Cope DW, Di Giovanni G, Fyson SJ, et al. Enhanced tonic GABAA inhibition in typical absence epilepsy. Nat Med 2009;15:1392–1398.
9. Huguenard JR, McCormick DA. Thalamic synchrony and dynamic regulation of global forebrain oscillations. Trends Neurosci 2007;30:350–356.
10. Paz JT, Davidson TJ, Frechette ES, et al. Closed-loop optogenetic control of thalamus as a tool for interrupting seizures after cortical injury. Nat Neurosci 2013;16:64–70.
11. Berényi A, Belluscio M, Mao D, Buzsàki G. Closed-loop control of epilepsy by transcranial electrical stimulation. Science 2012;337:735–737.
12. Cooper IS. Effect of chronic stimulation of anterior cerebellum on neurological disease. Lancet 1973;1:206.
13. Cooper IS, Amin I, Riklan M, et al. Chronic cerebellar stimulation in epilepsy. Clinical and anatomical studies. Arch Neurol 1976;33:559–570.
14. Cooper IS, Riklan M, Watkins S, McLellan D. Safety and efficacy of chronic stimulation. Neurosurgery 1977;1:203–205.
15. Dow RS, Smith W, Maukonen L. Clinical experience with chronic cerebellar stimulation in epilepsy and cerebral palsy. Electroencephalogr Clin Neurophysiol 1977;43:906.
16. Gilman S, Dauth GW, Tennyson VM, et al. Clinical, morphological, biochemical, and physiological effects of cerebellar stimulation. In: Functional electrical stimulation: applications in neural prosthesis. 5th ed. Hambrecht FT, ed. New York, NY: Marcel Dekker, 1977.
17. Levy LF, Auchterlonie WC. Chronic cerebellar stimulation in the treatment of epilepsy. Epilepsia 1979;20:235–245.
18. Bidziński J, Bacia T, Ostrowski K, Czarkwiani L. Effect of cerebellar cortical electrostimulation on the frequency of epileptic seizures in severe forms of epilepsy. Neurol Neurochir Pol 1981;15:605–609.
19. Wright GD, McLellan D, Brice JG. A double-blind trial of chronic cerebellar stimulation in twelve patients with severe epilepsy. J Neurol Neurosurg Psychiatry 1984;47:769–774.
20. Van Buren JM, Wood JH, Oakley J, Hambrecht F. Preliminary evaluation of cerebellar stimulation by double-blind stimulation and biological criteria in the treatment of epilepsy. J Neurosurg 1978;48:407–416.
21. Velasco F, Carrillo-Ruiz JD, Velasco M, et al. Double-blind, randomized controlled pilot study of bilateral cerebellar stimulation for treatment of intractable motor seizures. Epilepsia 2005;46:1071–1081.
22. De Zeeuw CI, Hoebeek FE, Bosman LWJ, et al. Spatiotemporal firing patterns in the cerebellum. Nat Rev Neurosci 2011;12:327–344.
23. Aumann TD, Horne MK. Ramification and termination of single axons in the cerebellothalamic pathway of the rat. J Comp Neurol 1996;376:420–430.
24. Teune TM, Van der Burg J, Van der Moer J, Ruigrok TJ. Topography of cerebellar nuclear projections to the brain stem in the rat. Prog Brain Res 2000;124:141–172.
25. Sawyer SF, Tepper JM, Groves PM. Cerebellar-responsive neurons in the thalamic ventroanterior-ventrolateral complex of rats: light and electron microscopy. Neuroscience 1994;63:725–745.
26. Sawyer SF, Young SJ, Groves PM, Tepper JM. Cerebellar-responsive neurons in the thalamic ventroanterior-ventrolateral complex of rats: in vivo electrophysiology. Neuroscience 1994;63:711–724.
27. Uno M, Yoshida M, Hirota I. The mode of cerebello-thalamic relay transmission investigated with intracellular recording from cells of

the ventrolateral nucleus of cat's thalamus. Exp Brain Res 1970;10: 121–139.

28. Shinoda Y, Futami T, Kano M. Synaptic organization of the cerebello-thalamo-cerebral pathway in the cat. II. Input-output organization of single thalamocortical neurons in the ventrolateral thalamus. Neurosci Res 1985;2:157–180.

29. Bava A, Manzoni T, Urbano A. Effects of fastiginal stimulation on thalamic neurones belonging to the diffuse projection system. Brain Res 1967;4:378–380.

30. Noebels JL, Sidman RL. Spike-wave and focal motor seizures in the mutant mouse tottering. Science 1979;204:1334–1336.

31. Fletcher CF, Lutz CM, O'Sullivan TN, et al. Absence epilepsy in tottering mutant mice is associated with calcium channel defects. Cell 1996;87:607–617.

32. Kandel A, Buzsáki G. Cerebellar neuronal activity correlates with spike and wave EEG patterns in the rat. Epilepsy Res 1993;16:1–9.

33. Tokuda S, Beyer BJ, Frankel WN. Genetic complexity of absence seizures in substrains of C3H mice. Genes Brain Behav 2009;8: 283–289.

34. Marescaux C, Vergnes M, Depaulis A. Genetic absence epilepsy in rats from Strasbourg—a review. J Neural Transm Suppl 1992; 35:37–69.

35. Kaplan BJ, Seyfried TN, Glaser GH. Spontaneous polyspike discharges in an epileptic mutant mouse (tottering). Exp Neurol 1979;66:577–586.

36. Hoebeek FE, Witter L, Ruigrok TJ, De Zeeuw CI. Differential olivocerebellar cortical control of rebound activity in the cerebellar nuclei. Proc Natl Acad Sci U S A 2010;107:8410–8415.

37. Loureiro M, Cholvin T, Lopez J, et al. The ventral midline thalamus (reuniens and rhomboid nuclei) contributes to the persistence of spatial memory in rats. J Neurosci 2012;32:9947–9959.

38. Holt GR, Softky WR, Koch C, Douglas RJ. Comparison of discharge variability in vitro and in vivo in cat visual cortex neurons. J Neurophysiol 1996;75:1806–1814.

39. Rasmussen CE, Williams CKI. Gaussian processes for machine learning. Cambridge, MA: MIT Press, 2006.

40. Bandt C, Pompe B. Permutation entropy: a natural complexity measure for time series. Phys Rev Lett 2002;88:174102.

41. van Dongen MN, Karapatis A, Kros L, et al. An implementation of a wavelet-based seizure detection filter suitable for realtime closed-loop epileptic seizure suppression. Paper presented at: Biomedical Circuits and Systems Conference (BioCAS), 2014 IEEE, pp. 504–507; October 22–24, 2014; Lausanne, Switzerland.

42. Osorio I, Frei MG, Wilkinson SB. Real-time automated detection and quantitative analysis of seizures and short-term prediction of clinical onset. Epilepsia 1998;39:615–627.

43. Karel JMH, Haddad SAP, Hiseni S, et al. Implementing wavelets in continuous-time analog circuits with dynamic range optimizatio-n.IEEE Trans Circuits Syst I 2012;59:229–242.

44. van Luijtelaar G, Onat FY, Gallagher MJ. Animal models of absence epilepsies: what do they model and do sex and sex hormones matter? Neurobiol Dis 2014;72(pt B):167–179.

45. van Luijtelaar G, Zobeiri M. Progress and outlooks in a genetic absence epilepsy model (WAG/Rij). Curr Med Chem 2014;21:704–721.

46. Akman O, Moshe SL, Galanopoulou AS. Sex-specific consequences of early life seizures. Neurobiol Dis 2014;72(pt B): 153–166.

47. Fisher RS, Velasco AL. Electrical brain stimulation for epilepsy. Nat Rev Neurol 2014;10:261–270.

48. Hoebeek FE, Khosrovani S, Witter L, De Zeeuw CI. Purkinje cell input to cerebellar nuclei in tottering: ultrastructure and physiology. Cerebellum 2008;7:547–558.

49. Hoebeek FE, Stahl JS, Van Alphen AM, et al. Increased noise level of Purkinje cell activities minimizes impact of their modulation during sensorimotor control. Neuron 2005;45:953–965.

50. Nathanson JL, Yanagawa Y, Obata K, Callaway EM. Preferential labeling of inhibitory and excitatory cortical neurons by endogenous tropism of adeno-associated virus and lentivirus vectors. Neuroscience 2009;161:441–450.

51. Polack PO, Charpier S. Intracellular activity of cortical and thalamic neurones during high-voltage rhythmic spike discharge in Long-Evans rats in vivo. J Physiol 2006;571:461–476.

52. Heckroth JA. Quantitative morphological analysis of the cerebellar nuclei in normal and lurcher mutant mice. I. Morphology and cell number. J Comp Neurol 1994;343:173–182.

53. Alva P, Kros L, Maex R, et al. A potential role for the cerebellar nuclei in absence seizures. BMC Neurosci 2013;14(suppl 1): 170.

54. Alva P, Kros L, Eelkman Rooda OHJ, et al. Combining machine learning and simulations of a morphologically realistic model to study modulation of neuronal activity in cerebellar nuclei during absence epilepsy. BMC Neurosci 2014;15(suppl 1):P39.

55. Rowland NC, Jaeger D. Coding of tactile response properties in the rat deep cerebellar nuclei. J Neurophysiol 2005;94:1236–1251.

56. Uusisaari M, Knopfel T. Functional classification of neurons in the mouse lateral cerebellar nuclei. Cerebellum 2011;10:637–646.

57. Bagnall MW, Zingg B, Sakatos A, et al. Glycinergic projection neurons of the cerebellum. J Neurosci 2009;29:10104–10110.

58. Aumann TD, Rawson JA, Finkelstein DI, Horne MK. Projections from the lateral and interposed cerebellar nuclei to the thalamus of the rat: a light and electron microscopic study using single and double anterograde labelling. J Comp Neurol 1994; 349:165–181.

59. Steriade M. Two channels in the cerebellothalamocortical system. J Comp Neurol 1995;354:57–70.

60. Andersen P, Eccles JC, Sears TA. The ventro-basal complex of the thalamus: types of cells, their responses and their functional organization. J Physiol 1964;174:370–399.

61. Destexhe A, Contreras D, Steriade M. Mechanisms underlying the synchronizing of corticothalamic feedback through inhibition of thalamic relay cells. J Neurophysiol 1998;79: 999–1016.

62. Zhang Y, Mori M, Burgess DL, Noebels JL. Mutations in high-voltage-activated calcium channel genes stimulate low-voltage-activated currents in mouse thalamic relay neurons. J Neurosci 2002;22:6362–6371.

63. Chan-Palay V. Cerebellar dentate nucleus: organization, cytology and transmitters. Heidelberg, Germany: Springer-Verlag, 1977.

64. Chow BY, Boyden ES. Optogenetics and translational medicine. Sci Transl Med 2013;5:177ps5.

65. Creed M, Pascoli VJ, Luscher C. Addiction therapy. Refining deep brain stimulation to emulate optogenetic treatment of synaptic pathology. Science 2015;347:659–664.

66. Krauss GL, Koubeissi MZ. Cerebellar and thalamic stimulation treatment for epilepsy. Acta Neurochir Suppl 2007;97:347–356.

67. Krook-Magnuson E, Szabo GG, Armstrong C, et al. Cerebellar directed optogenetic intervention inhibits spontaneous

hippocampal seizures in a mouse model of temporal lobe epilepsy. Eneuro 2014;1:1–15.

68. Engel J Jr. Outcome with respect to epileptic seizures. Milton J, Jung P, eds. New York, NY: Raven Press, 1987.

69. Chkhenkeli SA, Šramka M, Lortkipanidze GS, et al. Electrophysiological effects and clinical results of direct brain stimulation for intractable epilepsy. Clin Neurol Neurosurg 2004; 106:318–329.

70. Šramka M, Chkhenkeli IS. Clinical experience in intraoperational determination of brain inhibitory structures and application of implanted neurostimulators in epilepsy. Stereotact Funct Neurosurg 1990;54–55:56–59.

71. Šramka M, Fritz G, Galanda M, Nádvorník P. Some observations in treatment stimulation of epilepsy. Acta Neurochir (Wien) 1976; (23 suppl):257–262.

72. Fisher RS. Therapeutic devices for epilepsy. Ann Neurol 2012;71: 157–168.

73. Hartikainen KM, Sun L, Povivaara M, et al. Immediate effects of deep brain stimulation of anterior thalamic nuclei on executive functions and emotion-attention interaction in humans. J Clin Exp Neuropsychol 2014;36:540–550.